Paleoclimatic Response of the Closure of the Isthmus of Panama
in a Coupled Ocean-Atmosphere Model

by

Trevor Quentin Murdock
B.Sc., University of Victoria, 1995

A Thesis Submitted in Partial Fulfillment of the
Requirements for the Degree of
MASTER OF SCIENCE
in the School of Earth and Ocean Sciences

[redacted] We accept this thesis as conforming
to the required standard

[redacted]
Dr. Andrew J. Weaver, Supervisor (School of Earth and Ocean Sciences)

[redacted]
Dr. Chris Barnes, Departmental Member (School of Earth and Ocean Sciences)

[redacted]
Dr. Brian Bornhold, Departmental Member (Pacific Geoscience Centre)

[redacted]
Dr. Nigel Livingston, Outside Member (Department of Biology)

[redacted]
Dr. Harry Dosso, External Examiner (Department of Physics and Astronomy)

Supervisor: Dr. Andrew J. Weaver

ABSTRACT

The paleoclimatic effects of the closure of the Isthmus of Panama are investigated using a global, coupled atmospheric energy balance-ocean general circulation model. The Isthmus of Panama was a climatic, oceanographic, and biological forcing factor throughout the time of gradual closure (~ 12.5 – 2.5 Ma). A complete reconstruction of Isthmus closure is unavailable, but a synthesis of available studies shows response of different aspects of climatic and biological systems to different levels of closure. Hence, observations of (possible) effects of closure are spread throughout the Late Miocene and Pliocene.

The model Atlantic of the open Isthmus run is much fresher than in the present day run. Consistent with earlier ocean-only modelling studies, prior to closure there is an absence of deep water formation in the model North Atlantic. Hence, there is a reduction in oceanic heat transport and the model North Atlantic is significantly colder prior to Isthmus closure. Model runs with varying sill depth exibit unexpected changes in direction of Isthmus throughflow, with consequences for poleward heat transport. The utilization of an advective wind feedback is shown to make the thermohaline circulation less sensitive to the open Isthmus. Model runs with the Greenland-Scotland ridge closed emphasize the prime importance of a closed Isthmus of Panama in order for the model to exhibit active North Atlantic Deep Water production. The possibility of the thermohaline circulation response to Isthmus closure being related to Northern Hemisphere glaciation is examined.

An extensive model-data intercomparison is made. This comparison serves several purposes, in that it: (1) increases confidence in the sensitivity results (2) increases confidence in the use of the model for other applications (3) assists in addressing questions left open from observations alone and (4) assists in suggesting directions for potential future model studies.

In each case of model-observation intercomparison, the coarse model resolution as well as several other caveats, are kept in mind. This includes the fact that several other paleogeographic and paleoclimatic forcing factors were present during Isthmus closure that are not represented by the model. Also, the fact that examing the sensitivity to one change alone rules out the possibility of the model simulating any results that depended on a combination of factors is kept in mind. This means that the observational results are

relied on quite heavily, with the model used mainly to examine the feasibility of mechanisms suggested by observational studies, and to suggest what the next research steps might be. Such model-observation incomparison examples include the Late Miocene carbonate crash, tropical Pacific cooling, and Northern Hemisphere glaciation.

Examiners:

Dr. Andrew J. Weaver, Supervisor (School of Earth and Ocean Sciences)

[redacted]

Dr. Chris Barnes, Departmental Member (School of Earth and Ocean Sciences)

[redacted]

Dr. Brian Bornhold, Departmental Member (Pacific Geoscience Centre)

[redacted]

Dr. Nigel Livingston, Outside Member (Department of Biology)

[redacted]

Dr. Harry Dosso, External Examiner (Department of Physics and Astronomy)

Table of Contents

List of Tables

List of Figures

Glossary

Time

Ma	million years before present
ka	thousand years before present
Neogene	23.7 - 1.6 Ma
Late Miocene	11.2 - 5.3 Ma
Pliocene	5.3 - 1.6 Ma
Phanerozoic	570 Ma - present

Acronyms

IP	Isthmus of Panama
MM	Maier-Reimer *et al.*, 1990 and Mikolajewicz *et al.*, 1993
FW	Fanning and Weaver, 1996
OIP	open IP run
SIP	shallow sill run
MIP	mid-depth sill run
CTRL	present-day run
RBC	ocean-only restoring boundary conditions run
NWF	no wind feedback run
GSC	Greenland-Scotland ridge closed (IP closed also)
GSCOIP	Greenland-Scotland ridge closed with open IP
OGCM	ocean general circulation model
GCM	general circulation model
EMBM	energy-moisture balance model
ODP	Ocean Drilling Project
DSDP	Deep Sea Drilling Project
ENSO	El-Nino/Southern Oscillation

Glossary

Variables and parameters

SST	sea surface temperature
SSS	sea surface salinity
Q_T	eddy diffusive horizontal heat transport parameterization
Q_{LW}	net longwave emission to space
Q_{SSW}	scattering and absorption of incoming shortwave (eqn. 2)
Q_{RR}	longwave absorption and re-radiation over the oceans (eqn. 3)
C_0	reduction parameter representing clouds (eqn. 3)
Q_{SH}, Q_{LH}	sensible and latent heat fluxes
E	evaporation
P	precipitation
T_{SEA}	sea surface temperature
T_{AIR}	surface air temperature
q_{AIR}	surface specific humidity
C_E, C_H	bulk transfer coefficients (Dalton and Stanton numbers)
Q_{VM}	vertical-meridional oceanic heat transport in a given basin
V	depth-averaged northward transport in the thermocline
ΔT	temperature difference of thermocline and subthermocline water

Water masses and currents

NADW	North Atlantic Deep Water
AABW	Antarctic Bottom Water
AAIW	Antarctic Intermediate Water
NCW	Northern Component Water
NEC	North Equatorial Current
SEC	South Equatorial Current

Acknowledgments

I wish to extend sincere thanks to the many people that helped make my M.Sc. project possible. Particularly, I thank my supervisor, Dr. Andrew Weaver, for excellent guidance and support throughout the project. I am deeply grateful to Andrew for the opportunity to work with him and for his making it an incredible experience. I would consider it a privilege to collaborate with him, or work for him again in the future. I am also grateful for his friendship and hope that our families remain connected as well as our careers.

I wish to thank my committee members Drs. Chris Barnes, Brian Bornhold, Nigel Livingston, and Harry Dosso for their time on my committee. Also, I would like to thank Drs. Chris Barnes and Brian Bornhold for assistance in locating references.

I thank my family for their encouragement and support, and Tammy for enduring my "flexible" hours. Thanks to Rick Lee of the Canadian Institute for Climate Studies for flexibility regarding completion of the thesis after starting employment there. Thanks to all my colleagues and friends in the climate lab, particularly Dr. Augustus Fanning for demystifying the atmospheric model, and the immeasurable computer guru help from Daniel Robitaille.

I would like to acknowledge the School of Earth and Ocean Sciences, the University of Victoria, and the many people and institutions involved in the funding support of this project via scholarships and Teaching Assistantships to me and research grants to Dr. Andrew Weaver. Without this financial support the project would not be possible.

I must note the serendipity of Lindsey Murdock and Maria Weaver being born at virtually the same place and the same time. Without this event, I would never have asked Andrew what his research field was. I would not have known of the chance to work in an intriguing and stimulating field with a renowned and respected world-class researcher here in Victoria.

I thoroughly enjoyed my M.Sc., and am similarly enjoying my current employment at the Canadian Institute of Climate Studies that it led to. I finish by thanking my supervisor, Dr. Andrew Weaver, for leading me into the field of climate studies.

1 Introduction

The quest to understand the continual change of Earth's climate is an area of intense current research. New observations and modelling studies are increasing the understanding of past climates, which helps in the task of understanding how climate may change in the future. Models can contribute to identifying potential causes of climate change through sensitivity studies, and to understanding the coupled interactions between the ocean, atmosphere, cryosphere, and biosphere. Comparing results with past observations is also a good method of evaluating numerical models for use in present-day and future climate prediction applications (Kutzbach, 1992; Gates *et al.*, 1995).

The ocean, with its low albedo and large heat capacity is an important constituent of the global climate. The imbalance in solar radiation between the poles and equator drives major ocean circulations. The current continental configuration leads to a strong meridional component to the heat transport of the oceans. However, in the history of the oceans, there has not always been the zonal land barriers that exist today. There exist natural 'experiments' in earth's history, whereby changes in continental positions and oceanic gateways and ridges have occurred. Tectonic forcing by changes in oceanic gateways and ridges may be associated with several paleoclimatic observations (e.g., Berggren, 1982; Kennett,1982; Crowley and North, 1991; Wright and Miller, 1996). Modelling the ocean circulation subject to past tectonic changes provides an excellent avenue of investigation in order to understand past climate. The most recent zonal oceanic gateway change was the rise of the Isthmus of Panama (hereafter IP) from ~ 12.5 - 2.5 Ma. In this thesis, the effects on ocean circulation and global climate of an open IP are investigated through numerical modelling and comparison with observations. Particular attention is focused on the role of meridional heat transport by the ocean.

The rest of the introduction deals with details of IP closure, a brief outline of past studies, and a motivation of the approach taken in this study. The model utilized is described in §2. Numerical experiments and results are outlined in §3 and compared to data from regional (§4.1) and global (§4.2) observations. Finally, a summary and some concluding remarks are made in §5.

1.1 Paleogeography and chronology

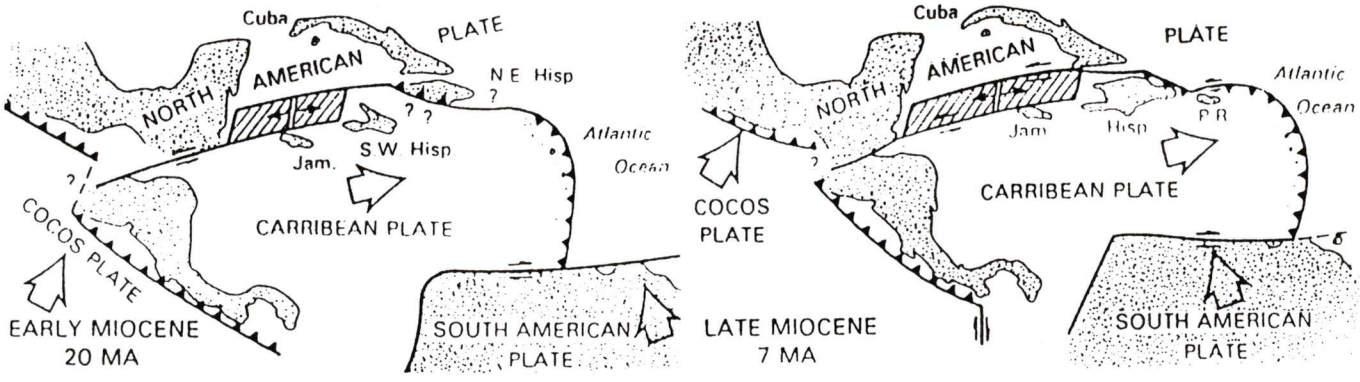

Figure 1.1.1: Central American paleogeography before and during Isthmus closure (taken from MM, originally from Sykes *et al.*, 1982).

Over 60 Ma ago, the Pacific plate began pushing the Cocos plate under the Caribbean plate (Figure 1.1.1). As the sinking plate melted, the molten rock emerged at the surface as a complex volcanic chain-island arc archipelago. This situation is similar to the formation of the chain of volcanoes (including Mt. St. Helens) resulting from the Juan de Fuca plate subducting under the North American plate. For the IP, the result was land formation where there had been ocean previously (Svitil, 1993; Collins *et al.*, 1996). The region of the IP is approximately 8-12°N, and 78-82°W (Figure 1.1.1). Other tectonic activity in the region may also have played a local oceanographic role, for example in the strengthening of the Gulf of Mexico Loop Current, the Caribbean Current, and the Gulf Stream (Droxler *et al.*, 1996). This study will focus on the major perturbation, IP closure, as it was certainly the most influential event at the time in terms of local, regional, and global effects on paleocirculation and potential effects on global climate and thus biota.

IP closure was gradual and perhaps intermittent. Different indicators have been found to respond to different levels of isolation of Pacific and Atlantic water. Gradual and intermittent closure coupled with sea level changes occurring throughout this time (Haq *et al.*, 1987) makes reconstruction of the evolution of the depth of the sill difficult. The chronology of closure is not well constrained, but increasing observations are improving the picture. A synthesis from a variety of sources is given below.

An analysis of Miami Terrace geology (Mullins and Neumann, 1979) suggests a submarine erosion ~16-10.5 Ma. Mullins and Neumann (1979) attribute this to initial IP closure via a postulated intensified Gulf Stream by diversion of Atlantic-Pacific throughflow into the North Atlantic. However, Mullins and Neumann (1979) admit that there is no a priori reason to expect that intensification of a surface current would cause erosion at depth. This erosion is more likely due to the increased thermohaline circulation observed at this time (Wright *et al.*, 1991), itself related to IP closure (§3.1, §4.2.1). Mullins and Neumann (1979) outlined results from several studies indicative of Mid-Miocene increased biological provinciality in the region of the IP, including analyses of radiolarians, molluscs, reefs, benthic foraminifera, and siliceous microfossils. These results may be indicative of an initial restriction of deepest throughflow by the Mid-Miocene.

Knowlton *et al.* (1993) found effects on snapping shrimp as early as ~12.5 Ma, as well as species divergences across the IP at 9.1-6.8, 6.3-4.0, and 6.1-4.4 Ma. Paleobathymetric analyses (Duque-Caro, 1990) and biostratigraphic evidence (Collins *et al.*, 1996) indicate at least three straits across the IP island arc, with a sill (~1000 m depth) at the Atrato strait by 10.4 Ma. This evidence indicates the presence of an Isthmus at ~8 Ma and both the Panama isthmian and San Carlos basin straits were closed, but the Atrato strait was ~200-750 m deep at this time. By ~6 Ma, the Panama isthmian strait shows a

return of shallow water flow of ~200-500 m depth, and the other two straits would have been deeper than this. The Atrato strait shoaled again to ~150 m by 5.3 Ma.

Ground sloths crossed from South to North America as early as 9.3-8.0 Ma, at a time when it is believed that islands had formed across the barrier and the sill was ~200 m (Marshall, 1985). Raccoons crossed from North to South America ~6.0 Ma. Benthic foraminiferal speciation and reef coral diversification in the Caribbean occurred ~8-6 Ma (Collins *et al.*, 1997). Gastropod divergence at the subgeneric level began as early as 5.0 Ma, culminating several Ma later (Jackson *et al.*, 1993). Planktonic foraminiferal results (Keller *et al.*, 1989) indicate increasingly restricted surface water exchange ~4.2 Ma, when marked salinity differences on either side of the IP are observed in stable isotopes (e.g., Keigwin, 1982). McDougall's (1996) analysis of benthic foraminifera with respect to water mass types is indicative of restriction of bottom water throughflow ~6.7 Ma, intermediate waters ~5.6 Ma, and surface waters from ~4.0-3.2 Ma.

Termination of shallow-water flow across the IP is found to occur ~3.5-3.0 Ma according to analyses of marine fauna (Coates *et al.*, 1992; Knowlton *et al.*, 1993). Several other analyses (Cd/Ca records: Delaney, 1990; carbon isotopes: Raymo *et al.*, 1992; sediment accumulation: Wold, 1994; and Nd, Pb, and Sr isotopic records: Burton *et al.*, 1997) are consistent with the time of ~4-3 Ma for final shallow water closure.

Planktonic (Keller *et al.*, 1989) and benthic (Crouch and Poag, 1979) foraminiferal data, as well as nannofossils (Gartner *et al.*, 1987) have been interpreted as suggestive of closure by 2.5 Ma, with some intermittent Pacific-Atlantic water communication until as late as 1.8 Ma. Most marine faunal evolutionary effects due to final uplift occurred ~2.4 Ma (see §4.1.4). Hence, only marine foraminifera and nannofossils were sensitive to this late connection, or evolutionary divergence was delayed due to some other ecological threshold until several 100 kyr after final closure at ~3-2.5 Ma. Perhaps the best measure

of final closure is the migration of land animals between North and South America which is dated at 2.9-2.5 Ma (Marshall, 1985; Vermeij, 1993).

1.2 Model-observation comparison

Gradual IP closure had various regional and perhaps global oceanographic, biological, and climatic effects. However, care must be taken not to attribute observations to IP closure as an excuse not to consider other factors which may have been important. Allmon *et al.* (1996) documented many effects of IP closure on biota off the Florida coast, but also found some changes that must be attributed to other factors. Studies of paleo records have led to many conclusions regarding the paleoceanography of the Late Miocene and Pliocene. These include the attribution of many observations to IP closure (§4).

In this thesis, some such results are analyzed, summarized, and compared to numerical modelling results (e.g., Murdock, Weaver, and Fanning, 1997). Since gradual IP closure is not very well constrained and because closure was gradual and perhaps intermittent (see §1.1 above), coincident timing is not enough to conclusively attribute data to IP closure. For example, one could assume observations from ~12.5-6 Ma should be attributed to initial closure, from ~8-5 Ma to deep water restriction, and from ~4-2.4 Ma to final shallow-water closure. There have certainly been other major climatic and oceanographic events during this time and there could be more as yet undocumented. Hence, mechanisms must also be found to link IP closure to "coincident" observations. Several authors have proposed mechanisms to explain a variety of causal links between IP closure, paleoclimate, and paleobiology. These mechanisms are often suggested by observations but difficult to support or deny further. Comparison to model results provides a potential avenue to assist in addressing the veracity of such proposed mechanisms and in pointing to appropriate directions for future research. In the comparison of data to model output below, a critical analysis will be made in each case in order to assess the relative

importance of IP closure to other potential forcing factors. Some of the other changes taking place during the time of closure include gradual Cenozoic cooling, Iceland ridge subsidence, volcanism, sea level fluctuations, isolation of the Mediterranean, changes to the Asian monsoon, orogeny, CO_2, closure of the Indonesian seaway, opening of Bering Strait, changes to the Greenland-Scotland ridge, initial ice sheet formation on Greenland, changes in Southern Hemisphere glaciation, and vegetation changes.

While model-observation comparison does provide another clue to the puzzle, it is not without its own challenges. An important one is the selection of an appropriate model. Ocean-only models (Maier-Reimer *et al.*, 1990; Mikolajewicz *et al.*, 1993—hereafter referred to as MM) have been used previously. In this thesis, data are compared to numerical results from a coupled model with a simple atmosphere, a particularly appropriate model for process-oriented paleoclimatic sensitivity studies (Fanning and Weaver, 1996—hereafter FW; Murdock, Weaver, and Fanning, 1997; Fanning, 1997).

The biggest hurdle in comparing observations to numerical model results comes from incompatible temporal and spatial scales. Observations come chiefly from fossil records and oceanic cores at specific locations, and many local effects of IP closure in the equatorial Atlantic and Pacific are well documented. Coarse model resolution hinders comparison to these observations of local effects — comparison is more appropriate on larger regional or global scales.

Temporally, observations span the entire time of IP closure, a period of ~10 Ma, with small scale fluctuations resolved. For example, data suggesting changes to upwelling throughout the time of IP closure (Pujos, 1987; §4.1.3) indicate that the largest changes in upwelling and surface currents occurred while the IP was closing, and that the two end states are not so different from each other. Pujos attributes all of these changes to IP closure. The model, on the other hand, is a sensitivity to a perturbation, in which other

global changes during the period of actual closure have been neglected. Thus, the open IP model run (termed OIP), which has a sill depth corresponding to the situation prior to ~12.5 Ma, is not representative of the climate prior to 12.5 Ma. However, the difference between the present-day run (termed CTRL) and OIP should provide a good representation of the change in mean climate between 12.5 Ma and today that can be attributed to IP closure alone.

To address this discrepancy, two additional model runs were made (Figure 1.2.1), each with different sill depths. A middle depth run (MIP) has a sill depth (1350 m) corresponding roughly to ~10 Ma, when the IP was cut off to deep water, and the shallow run (SIP, 200 m) to ~3.5 Ma, just prior to closure. The subtle point regarding which run to compare to, and whether other major differences occur in the observations that were not modelled, must be kept in mind when making model-observation comparisons.

IP closure is recent enough that there is a significant amount of data to compare with model results. IP observations include biostratigraphy, vertebrate and invertebrate fossils such as corals, planktic and benthic foraminifera and radiolaria, extinctions, isotopes, near-shore marine records and ocean sediment cores. Individual references to other changes during closure and to sources of observations will be made below as they come into discussion. The sensitivity approach of only changing the gateway holds better for the time of IP closure than for other less recent major gateway changes. For example, during the Drake Passage closure ~40-30 Ma, there was a much smaller Atlantic basin and other major geographical differences such as changes in ocean ridges. Ocean-only general circulation model (OGCM) studies on Drake Passage (e.g., Mikolajewicz, Maier-Reimer *et al.*, 1990, 1993) have not tried to incorporate these differences, which may be large enough to have significant effects even on sensitivity results.

Overview of Model Runs:

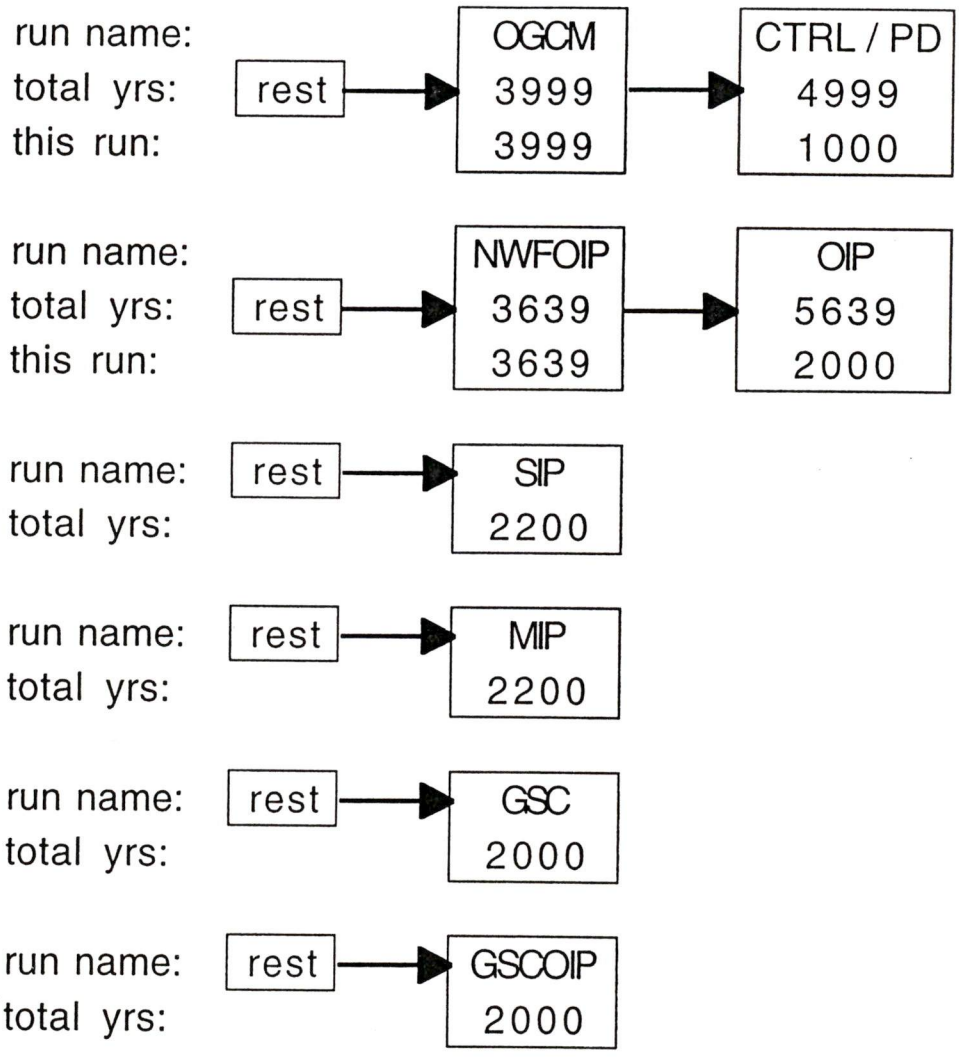

Figure 1.2.1: Schematic of numerical experiments carried out. Rest refers to starting the model from homogeneous conditions at year 0. Total yrs refers to the end year of the integration since beginning from rest. This run refers to the length of integration with a particular model configuration. Run details are: RBC: ocean-only Restoring Boundary Conditions; CTRL: present day (ConTRoL run); NWF: No Wind Feedback; OIP: Open IP (deep); SIP: Shallow IP sill open; MIP: Mid-depth IP sill open; GSC: Greenland-Scotland ridge Closed (IP closed also); GSCOIP: Greenland-Scotland ridge Closed with Open IP.

1.3 Previous model results

The OIP sensitivity has also been performed with OGCMs (e.g., MM). However, ocean-only models lack atmosphere-ocean feedbacks. Also, relaxation to present day ocean temperature and salinity fields is required as data on past fields are too sparse. Hence, results are biased towards present day climatology. Furthermore, no atmosphere-ocean feedbacks are present in OGCMs. Both of these factors could be very important to the IP sensitivity results.

Nevertheless, OGCM deep circulation results tend to agree with observations in several respects (MM). For example, the modelled global overturning streamfunction is consistent with observations (e.g., Kaneps, 1979; Brunner, 1983/84) which suggest a strengthened overturning after the IP closed. However, relaxation boundary conditions to present climatology could restrict modelled poleward heat transport from responding to a change in a sensitivity as surface heat flux is largely dependent on air-sea interactions.

Atmospheric GCMs coupled to OGCMs are complex and computer resource intensive in order to fully represent atmospheric processes. Furthermore, although they do not require relaxation boundary conditions, they do require flux adjustments to prevent climate drift (Weaver and Hughes, 1996), which is unphysical and also results in present day bias.

1.4 Purpose of study

The role of atmosphere-ocean feedbacks and modern day bias (from restoring boundary conditions) is potentially a very important one, particularly for the thermohaline circulation. Hence, this study re-examines the IP sensitivity via numerical experiments performed with a realistic geometry, global atmospheric energy moisture balance model (EMBM) coupled to a thermodynamic ice model and an OGCM. Particular attention is

focused on the effects of the thermohaline circulation. Because the use of the EMBM differentiates this study from previous IP sensitivity analysis, it is outlined in more detail than the other model components (§2). Some simple atmospheric diagnostics unavailable from ocean-only studies are also analyzed. A focus is made here on intercomparison between data and model results, as this has not been addressed to any detail in past studies (MM), and is important for the reasons outlined in §1.2 above.

2 Model description

2.1 Atmosphere

The atmospheric EMBM was designed (by Augustus Fanning and Andrew Weaver at the University of Victoria—FW; Fanning, 1997) as a simple, inexpensive (on computer resources) model which relates the evolution of the atmosphere to sea-surface temperature (SST), surface air temperature, and surface humidity only. Many assumptions must be made in the EMBM equations and parameterizations in order to make such a simplification of atmospheric processes. The parameterizations are discussed in more detail in §2.3. One major basic assumption which the model relies on is that the scales of interest here are interannual and longer in time and >1000 km in space. This allows assumption of diffusive transport since the atmospheric advective transports occur over time scales much faster in comparison (Lorenz, 1979). Furthermore, the land mass can be assumed to have no moisture or heat storage, hence no latent and sensible heat fluxes, on such large time scales.

The atmospheric energy balance is given as:

$$\rho_{AIR}\, C_{pa}\, H_{AIR}\, (dT_{AIR}/dt) = Q_T - Q_{LW} + Q_{SSW} + Q_{RR} + Q_{SH} + Q_{LH} \qquad (1)$$

where ρ_{AIR} is a constant surface air density, C_{pa} is the specific heat of air at constant pressure, H_{AIR} is a constant height scale for the atmosphere (Gill, 1982), and T_{AIR} is the surface air temperature.

Q_T is given by an eddy diffusive horizontal heat transport parameterization which incorporates a latitudinally dependent heat transport coefficient, ν, meant to represent processes associated with baroclinic eddies and the Hadley Cell (Lindzen and Farrell, 1977).

The net longwave emission to space, Q_{LW}, is calculated by a clear-sky empirical formula devised by Thompson and Warren (1982) specifically for use with low-resolution vertically-averaged models (it relies only on surface temperature and height-mean relative humidity). They present arguments for neglecting surface elevation, surface emissivity, temperature discontinuity at the surface, and distribution of carbon dioxide (a constant concentration with height is assumed) in the parameterization due to each parameter being either fairly constant or not significantly affecting Q_{LW}. The use of this parameterization allows for the water vapour-planetary longwave feedback.

Q_{SSW} is a source term in the atmosphere which represents the scattering and absorption of incoming shortwave by water vapour, dust, ozone, and clouds. Specifically:

$$Q_{SSW} = (S_0/4)\, S\, (1-\alpha)\, (1-C_0) \qquad (2)$$

where S_0 is the solar constant, S is the annual distribution of heat flux entering the atmosphere (North, 1975), α is the albedo, and C_0 is a reduction parameter representing the scattering and absorption processes discussed above.

Greenhouse gas absorption and longwave re-radiation over the oceans is given by:

$$Q_{RR} = \varepsilon_O\, \sigma\, (T_{SEA})^4 - \varepsilon_A\, \sigma\, (T_{AIR})^4 \qquad (3)$$

where T_{SEA} is the sea surface temperature, ε_O and ε_A are the oceanic and atmospheric emissivities, respectively, and σ is the Stefan-Boltzmann constant.

The fitting of COADS and Levitus observations to the EMBM equations is used to determine ε_A and C_0. These parameters generally agree with other estimates, although some differences are present (see FW). An inverse method based on North Atlantic Ocean data (Isemer *et al.*, 1989) is used to obtain ε_0. The albedo is determined from clear-sky ERBE data (Graves *et al.*, 1993). The bulk transfer coefficients (Dalton and Stanton numbers, C_E and C_H) are taken as a best linear fit to wind speed and air-sea temperature difference, rather

than simply using constants. Zonally-averaging these coefficients for the EMBM climatology gives values consistent with observational estimates.

Traditional bulk parameterizations (see FW for equations not shown here) are employed for the sensible and latent heat fluxes, Q_{SH}, Q_{LH}, as well as for the evaporation, E. Precipitation, P, is calculated by reducing relative humidity to 85% whenever it exceeds this value.

The atmospheric moisture balance is given as:

$$\rho_{AIR} H_q (dq_{AIR}/dt) = M_T + (\rho_{SEA} / syr) (E - P) \qquad (4)$$

where syr is the number of seconds per year, q_{AIR} is surface specific humidity, and H_q is a constant height scale for the atmosphere (Gill, 1982).

M_T is an eddy diffusive approximation which incorporates a horizontal redistribution parameter, κ, obtained by fitting the steady state, zonally averaged equation to observational estimates of E-P. The zonal-mean transport is comparable to observations polewards of about 20°, but transport in the Inter-Tropical Convergence Zone cannot be represented by down-gradient diffusion. This method leads to deficiencies in the hydrological cycle, but it does retain the main feedback mechanism.

A simple wind feedback, which consists of calculating anomalous winds from surface pressure fields, is also utilized. The use of eddy-diffusion rather than advection also contributes to the smoothness of modelled fields (e.g., Figure 3.1.5). Since we assume no heat or moisture storage on land, Q_{SH} , Q_{RR}, and E are zero there. P over land is simply returned to the ocean via a river mask (§2.4). Over land, the surface albedo is increased by 0.105 if the air temperature falls below -10°C, to parameterize the effect of snow cover.

Uncertainty in the model parameters is difficult to ascertain. Many observations were used but data analysis and collection problems contain biases and uncertainties. FW performed parameter sensitivity experiments whereby each parameter was adjusted by

±40% of their values. Within the context of the uncertainty in each parameter, the largest sensitivity was in C_0 (i.e. the effects of clouds are poorly represented), but resulted in a maximum equatorial temperature difference of only 0.7°C, within ship based uncertainty (Blanc, 1987). The use of the EMBM for climate variability studies (FW) indicates that the robust model climatology is not simply due to it being constrained by observationally-based parameterizations.

2.2 Ocean and ice

The atmospheric model was coupled to a modified version of the Geophysical Fluid Dynamics Laboratory Modular Ocean Model OGCM version 1.1 (Pacanowski *et al.*, 1993). All of the models were run at a coarse resolution of 1.855° latitude by 3.75° longitude. The OGCM has 19 vertical levels of varying depth (from 25 m to 600 m), and constant vertical diffusivity of 0.3 cm^2/s. The OGCM was run with implicit vertical mixing and instantaneous convection when the water column becomes unstable (see Weaver and Hughes, 1996).

The OGCM suffers from deficiencies common to all coarse-resolution OGCMs: misrepresentation of mixing and convection yielding a thermocline which is too diffuse, western boundary currents which are too wide and too weak, and a meridional heat transport which is too low. The modelled deep circulation is consistent with observations and OGCM results.

The ice model (coupled in as a component of the atmospheric model) includes brine rejection during ice growth as well as the insulating effect of ice cover (Semtner, 1976). It has no representation of snow on ice, sea ice dynamics, or leads.

2.3 Discussion

The EMBM was not designed to be a complete representation of the atmosphere. However, when compared to boundary conditions used in OGCMs, it is more physically-based, retains important feedback mechanisms, and some simple atmospheric diagnostics can be performed. All parameters in the EMBM are zonally averaged, due to the focus on model simplicity. Although this neglects several processes that could in fact be represented, FW argue that such 'fine tuning' would limit the usefulness of the model over a wide range of applications. Indeed, retaining the simple latitudinal profiles allows less modern climate bias than otherwise would occur, although some is inevitable since paleodata are too sparse to base empirical parameterizations on them. Misrepresentation of clouds includes their effects on albedo (the planetary albedo is parameterized by a clear-sky approximation, as is the outgoing IR). The model does, however, retain a water vapour feedback. Use of bulk parameterizations affects the calculation of E and P, and hence the hydrological cycle. Since fine tuning of C_E and C_H in the parameterization can constrain the heat flux, an adaptive best-fit approach is used. The most poorly modelled term is hence the latent heat, Q_{LW}, which Isemer *et al.* (1989) show has the largest uncertainties in observationally-based poleward heat transport estimates as well.

For present purposes, systematic errors in the latent (and sensible) heat fluxes mainly impede the comparison of model results to ocean heat transport measurements. However, comparison of estimates by different methods (e.g., between direct and indirect) is already problematic (e.g. Talley, 1984). Furthermore, both OGCMs and fully coupled models underestimate poleward heat transport in comparison to observations by a factor of one half, a persistent problem in ocean modelling. Nevertheless, a comparison between model climatologies with and without the IP should be robust. Indeed, the sensitivity results in Murdock, Weaver, and Fanning (1997) are consistent with observations even though absolute magnitudes of present heat transport are roughly half of Bryden's (1993)

direct estimate. Furthermore, FW show that the EMBM is suitable for sensitivity studies over a wide range of climatologies by showing that results (in this case the EMBM response to interpentadal changes in SST) are robust even if the reference state is dramatically altered by changing values of parameters. Fanning and Weaver (1997a) have also successfully applied this model to the Younger Dryas period (~11 ka), under different climatological conditions from present as well other modelling applications including studies of horizontal resolution and diffusion (Fanning and Weaver, 1997b) and flux adjustments (Fanning and Weaver, 1997c).

The strengths of the model include its simplicity, applicability under different climatic conditions, and avoidance of flux adjustments upon coupling. One example where the coupled EMBM outperforms stand-alone OGCMs under restoring boundary conditions and coupled GCMs with flux corrections is the avoidance of a diffuse thermocline and warm deep ocean bias common to these other models. Also, incorporation of the thermodynamic ice model allows realistic temperatures under ice rather than "spiking" the data to avoid fair weather bias.

Both decadal variability and multiple equilibria have been found to be possible in the coupled model under certain conditions (FW; Fanning and Weaver, 1997b). No evidence of either decadal variability or multiple equilibria was found in any of the IP integrations.

2.4 Experiments and coupling

The various model runs are depicted in Figure 1.2.1. All runs start initially from homogeneous resting conditions. The ocean model is run to equilibrium (RBC - 4000 years of integration of the OGCM under restoring boundary conditions). This run is then coupled to the atmosphere and ice models and run to its equilibrium (1000 years), in order

to obtain the present-day climatology of the coupled model (CTRL - §3.1). The perturbation runs are obtained by integrating the coupled model for at least 2000 years with the appropriate change in topography present from the start. The no-wind-feedback run (NWF) is obtained by integrating for about 3600 years with an open IP (deepest sill). The OIP run with wind feedback now included is then obtained by integrating from the end of the NWF run.

Other details of model coupling and results can be found in FW. Note that the model coupling requires a method for handling precipitation over land. The simplest approach is taken, whereby precipitation over land is instantaneously returned to the ocean. This approximation should be valid on the time and length scales of consideration here. Note that the land mass used roughly represents an effect of modern orography via present-day drainage basins (Weaver and Hughes, 1996). An attempt to simulate drainage basins more representative of the time period of the sill depth of the runs would be problematic due to data sparcity and gradual closure, and hence introduce an unknown perturbation to the results. Thus, for this sensitivity study, the runoff scheme is held constant throughout all the runs. This should not be taken as an assumption that no major changes in river runoff have occurred since this time, they have (e.g., Hoorn *et al.*, 1995). For regional results, errors due to this approximation would be expected to be small, and upon subtraction from the control run (CTRL), this effect will be assumed negligible.

3 Model results

3.1 Sensitivity to closure (CTRL, OIP)

A detailed present-day model climatology (CTRL) discussion can be found in FW. Here, CTRL results will be presented only for purposes of comparison to OIP. The CTRL climatology will also be inherent in difference plots, although the actual CTRL absolute fields may not always be shown. FW show that the model present-day climatology is in good general agreement with today's observed climate.

Associated with an open IP are differences in biological lifeforms, homogenization of tropical Atlantic and Pacific water properties, lack of NADW formation, and other effects noted below. Today, the trade winds carry a one-way freshwater flux from the Atlantic to Pacific across the narrow land bridge, but there are large temperature, salinity, and life form differences on either side of the IP. Before closure, water was able to flow in either direction through the IP, which allowed Atlantic and Pacific water in the region to mix properties. Many authors (e.g., Berggren and Hollister, 1974; Mullins and Neumann, 1979; Kennett, 1982; Pujos, 1987; Svitil, 1993; Lyle *et al.*, 1995; Gore, 1997) have assumed that this current was Atlantic-to-Pacific, what remained of the Tethys circulation, as suggested by a laboratory study (Luyendyk *et al.*, 1972). In contrast, for the OIP run, higher Pacific dynamic height (not shown) drove a Pacific-Atlantic IP net throughflow of 15.6 Sv (Figure 3.1.1). Regional marine biostratigraphic evidence is also indicative of Pacific-Atlantic throughflow (e.g., Collins *et al.*, 1996).

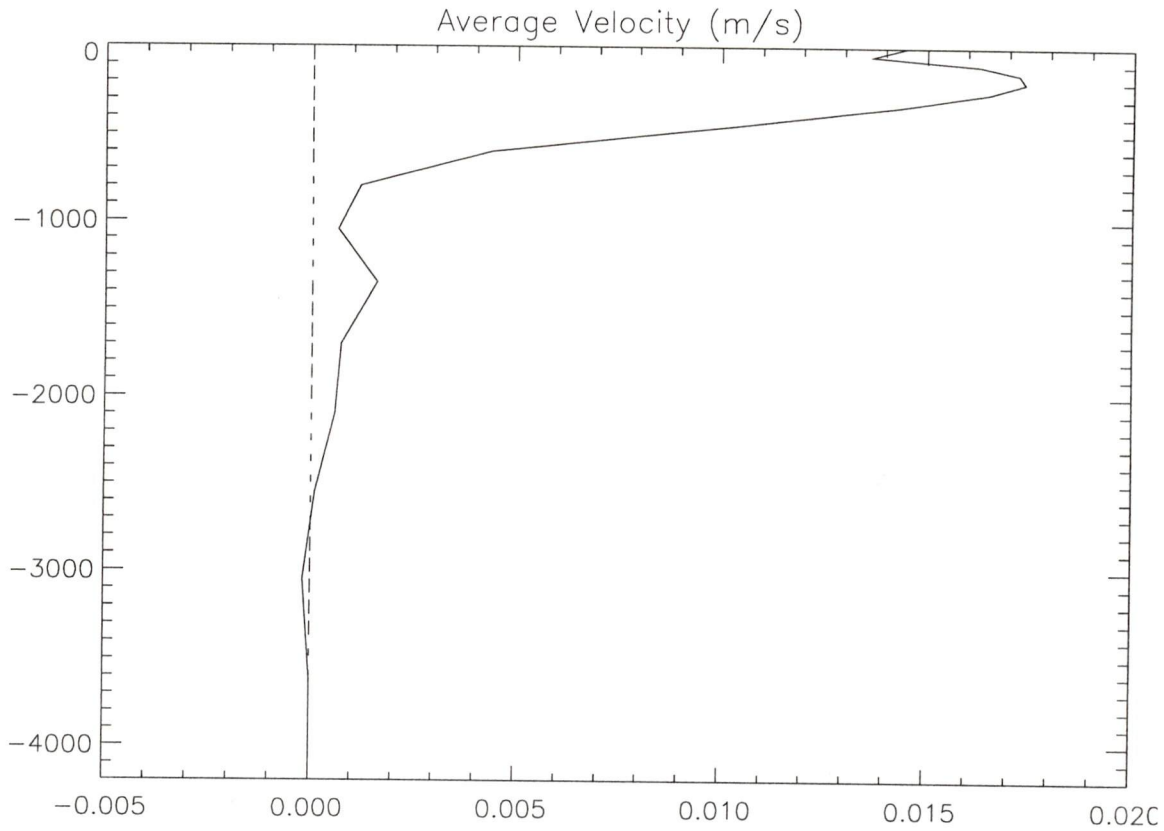

Figure 3.1.1: Vertical profile of flow through the Isthmus of Panama. Positive indicates Pacific to Atlantic throughflow.

Gradual cessation of fresh Pacific IP flow into the Atlantic is seen in planktonic foraminifera stable isotope trends for the Caribbean and East Pacific sites from ~6-2 Ma, which are suggestive of gradually increasing Caribbean sea surface salinity (SSS) from ~4 Ma (Keigwin, 1982). This SSS change was responsible for the gradual evolutionary increase in salinity tolerant species in the Caribbean from 4.2-2.4 Ma (Keller *et al.*, 1989). These observations compare favourably with modelled change in SSS (Figure 3.1.2). With the IP open, North Atlantic SSS is decreased to the extent that North Atlantic waters are so fresh that sinking is inhibited and NADW production does not occur (Figure 3.1.3). This result supports the prime importance of North Atlantic salinity to an active thermohaline circulation (Warren, 1983).

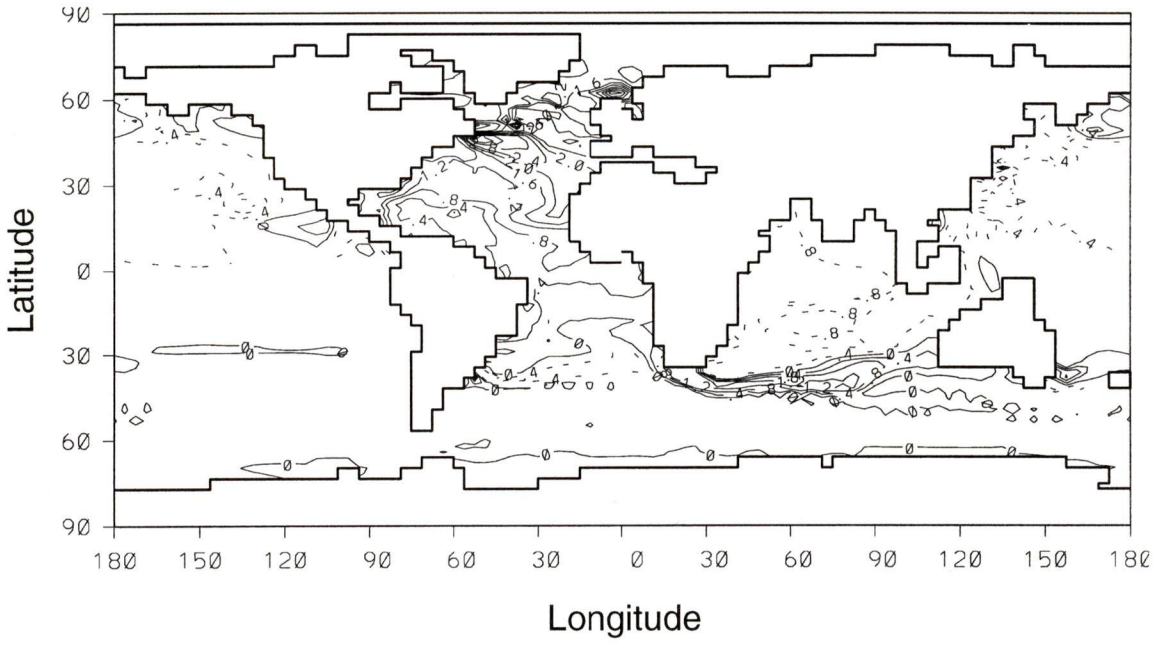

Figure 3.1.2: Sea surface salinity difference between the present day and open Isthmus runs (CTRL-OIP). Positive represents salinity increasing as the Isthmus closed (fresher when the Isthmus was open). Contour interval is 0.4 psu.

The state of collapsed NADW is a stable mode equivalent to the Southern Sinking state found by Manabe and Stouffer (1988). Associated with the lack of NADW prior to IP closure, is a reduction in oceanic heat transport (both global and Atlantic – Figure 3.1.4; Table 1), resulting in colder North Atlantic surface air temperatures (Figure 3.1.5). This modelled warming upon the closure of the model IP seems appropriate for comparison to the reconstructed warm period of ~3 Ma from ODP results by Dowsett *et al.* (1996). Figures 5a and b also show that with the IP open, slightly more AABW and Antarctic Intermediate Water production occurs. IP closure may also be linked indirectly to the onset of Northern Hemisphere glaciation (§4.2.4).

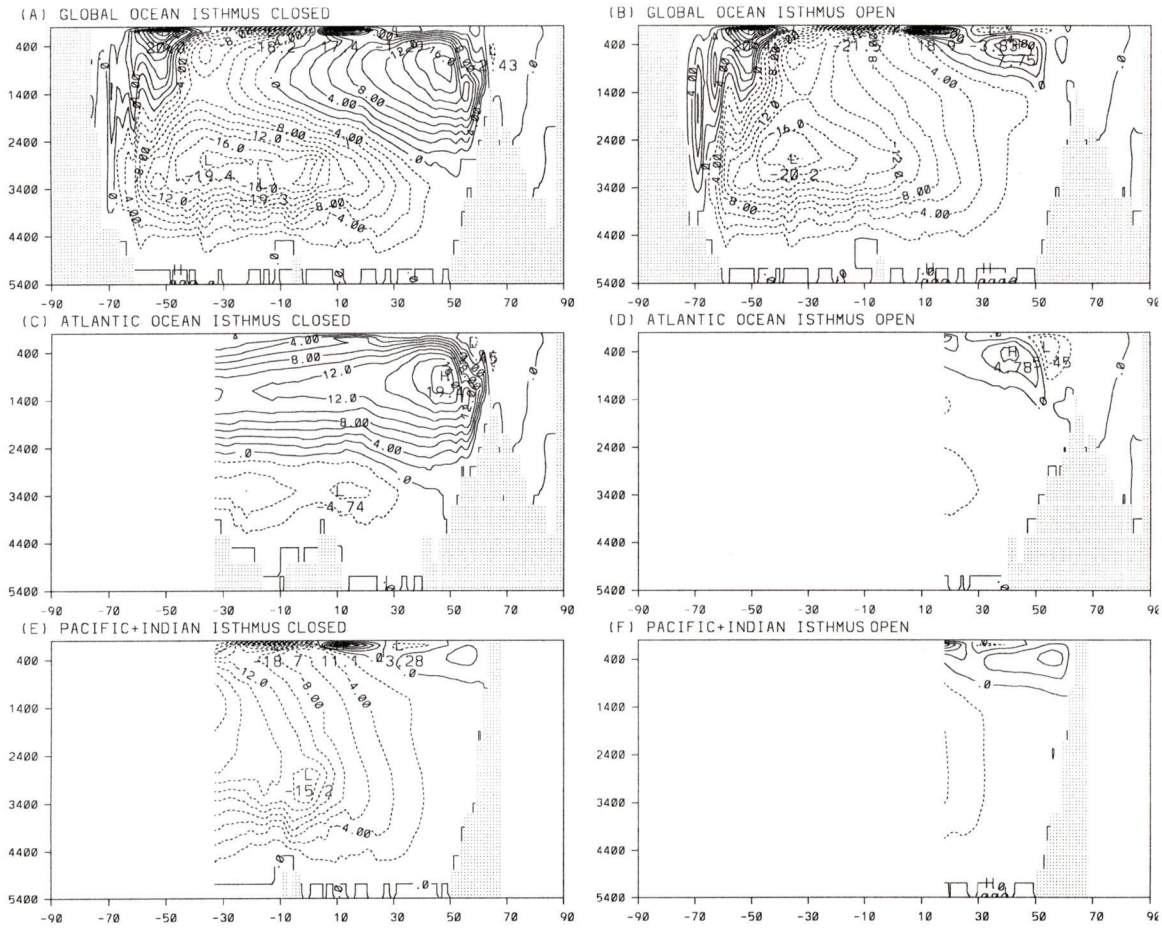

Figure 3.1.3: Global meridional overturning streamfunction (in Sv = $10^6 m^3 s^{-1}$) from the equilibrium climate in the case with: (a) Isthmus closed (present day CTRL) (b) Isthmus open (OIP). Atlantic: (c) CTRL (d) OIP. Pacific: (e) CTRL (f) OIP. The contour interval is 2 Sv in all cases and positive contours indicate clockwise circulation. Since it is only possible to define an overturning streamfunction in individual basins where there is land on both the eastern and western boundaries, the Atlantic and Pacific overturning plots are cut off at the tip of Africa (c, e) or at the Isthmus (d, f).

Table 3.1.1: Comparison of Oceanic Poleward Heat Transports

Observations (Bryden, 1993)	Global	Atlantic	Pacific	Global	Atlantic	Pacific
Vertical-meridional	1.66	1.28	0.38	0.84	0.65	0.19
Horizontal	0.32	-0.06	0.38	0.16	-0.03	0.19
Total	**1.98**	1.22	0.76	1.00	0.62	0.38
Model Isthmus-closed	Global	Atlantic	Pacific	Global	Atlantic	Pacific
Vertical-meridional	0.90	0.73	0.17	0.82	0.66	0.15
Horizontal	0.20	0.03	0.17	0.18	0.03	0.15
Total	**1.10**	0.76	0.34	1.00	0.69	0.31
Model Isthmus-shallow	Global	Atlantic	Pacific	Global	Atlantic	Pacific
Vertical-meridional	0.61	0.62	-0.02	0.77	0.68	-0.02
Horizontal	0.16	0.05	0.26	0.23	0.06	0.28
Total	**0.92**	0.67	0.25	1.00	0.73	0.27
Model Isthmus-middepth	Global	Atlantic	Pacific	Global	Atlantic	Pacific
Vertical-meridional	0.06	0.10	-0.03	0.13	0.20	-0.07
Horizontal	0.43	0.10	0.32	0.87	0.21	0.66
Total	**0.49**	0.20	0.29	1.00	0.41	0.59
Model Isthmus-deep	Global	Atlantic	Pacific	Global	Atlantic	Pacific
Vertical-meridional	0.54	0.26	0.28	0.77	0.37	0.40
Horizontal	0.16	-0.05	0.21	0.23	-0.07	0.30
Total	**0.70**	0.21	0.49	1.00	0.30	0.70

Oceanic poleward heat transport (in Petawatts; 1PW $\equiv 10^{15}$ W) at 24°N from the observations of Bryden (1993) and for the coupled model equilibrium climatologies with the Isthmus of Panama both open and closed. Columns 2 through 4 give the heat transport in the Global, Atlantic and Pacific Oceans, respectively. These transports have been normalized in columns 5 through 7 by the total global transport highlighted in bold in column 2. The poleward heat transport has further been partitioned into two subcomponents following the terminology of Bryden (1993): The vertical-meridional overturning which includes the wind-driven Ekman component is defined as $\rho C_P \int \langle v(z)\rangle\langle\theta(z)\rangle L(z)dz$, and the horizontal component as $\rho C_P \iint (v-\langle v\rangle)(\theta-\langle\theta\rangle)dxdz$. Here L(z) is the width of the basin at each depth z; v is the meridional velocity; x is the zonal coordinate (positive eastward); θ is the potential temperature; ρ is the density; C_P is the specific heat of seawater; < > denotes a zonal average across the basin.

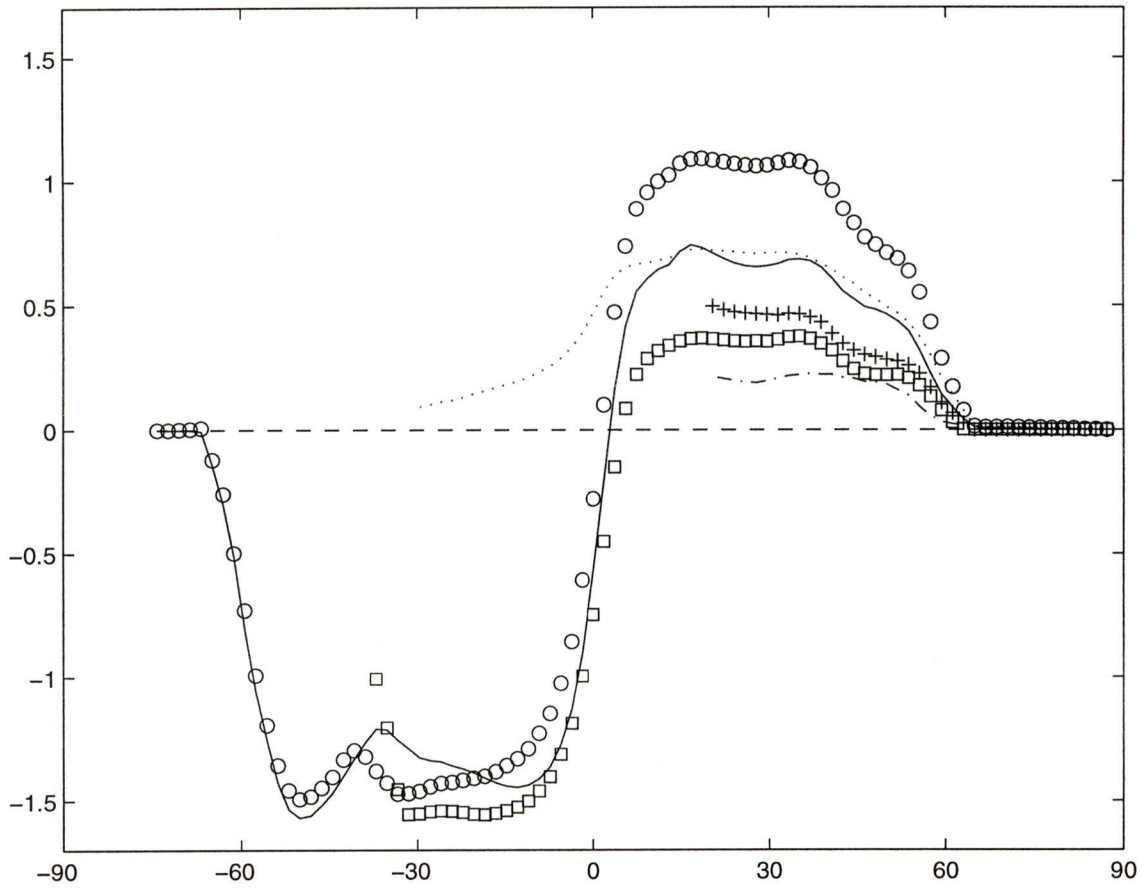

Figure 3.1.4: Oceanic heat transport (in PW ≡ 10^{15} Watts) as a function of latitude from the equilibrium climate of the coupled model simulations. The present day (CTRL) Global, Atlantic and Pacific+Indian Ocean transports are indicated by the o, ..., and lines, respectively. The open Isthmus (OIP) transports for the Global, Atlantic and Pacific Oceans are indicated by the —, _., and + lines, respectively.

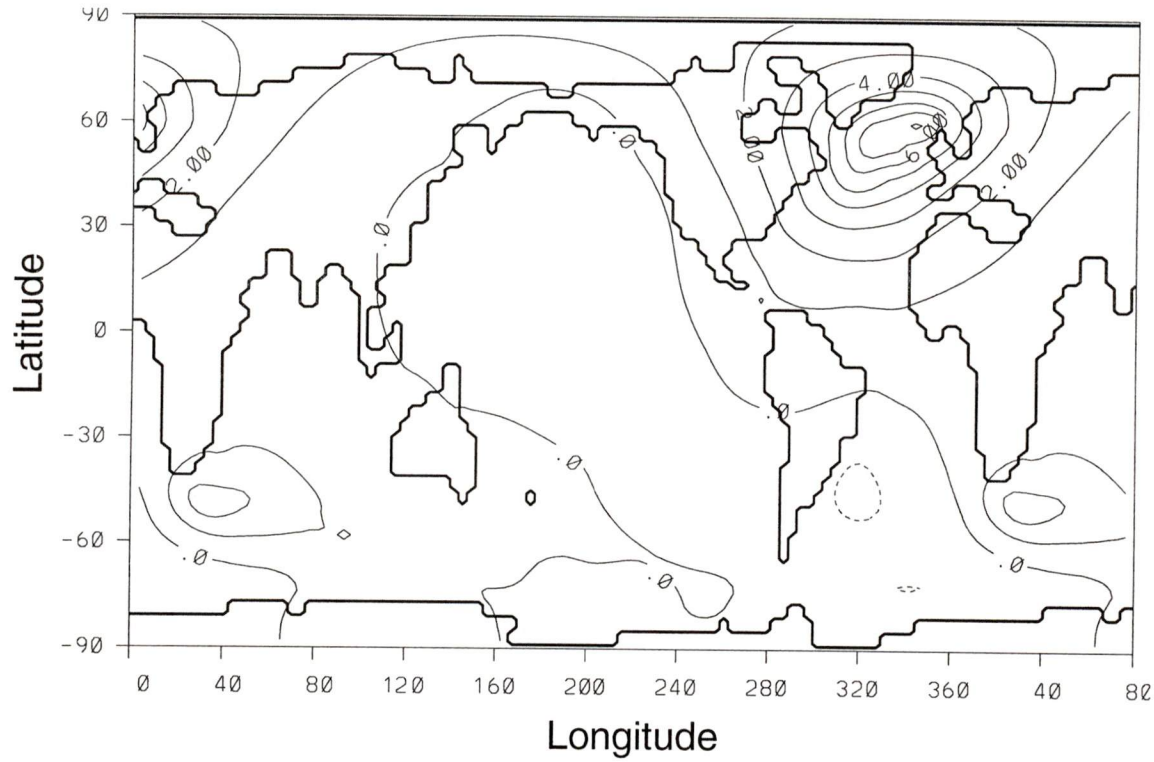

Figure 3.1.5 Global surface air temperature difference (°C) between the present day and open Isthmus of Panama equilibrium climatologies (CTRL–OIP). The contour interval is 1 °C.

3.2 Sill depth experiments (MIP, SIP)

The main sensitivity run described in the last section was made with a very deep sill (~ 3600 m), in order to determine a sensitivity to the open IP in the model. For the mid-depth run and shallow runs, MIP and SIP, the sill was imposed at uniform 1350 m and 200 m depths, respectively. The depths are roughly representative of ~10 Ma and ~4 Ma, respectively. The model Isthmus is still open to a greater latitudinal extent than it was at these times. Everything else held fixed in the OIP run was also held fixed for these runs (e.g., runoff mask). Hence, these runs should also be viewed as further sensitivity studies regarding the effects of sill depth rather than a simulation of time slices.

The transport through the sill for the MIP case is shown in Figure 3.2.1. The MIP net transport is virtually 0 Sv with 6 Sv entering the Atlantic from the Pacific near the

surface (~ 300 m) and 6 Sv returning at mid-depth (~ 1000 m). The reduction in net transport with decreasing sill depth reduces the level of homogenization of water properties on either side of the sill. As the sill depth reduces in the model from OIP to MIP, the North Atlantic SSS becomes slightly more saline. Consequently, the Gulf Stream intensifies, NADW production begins to strengthen (Figure 3.2.2), and poleward heat transport increases (Table 1) with global effects on surface temperatures (Figure 3.2.3). These figures demonstrate that the significant level of exchange of Atlantic and Pacific waters is still able to cause a major difference in global climate variability, even though there is no large net transport (as there is in the deep sill OIP case). These results will be further analyzed and compared to regional (§4.1) and global (§4.2) observations.

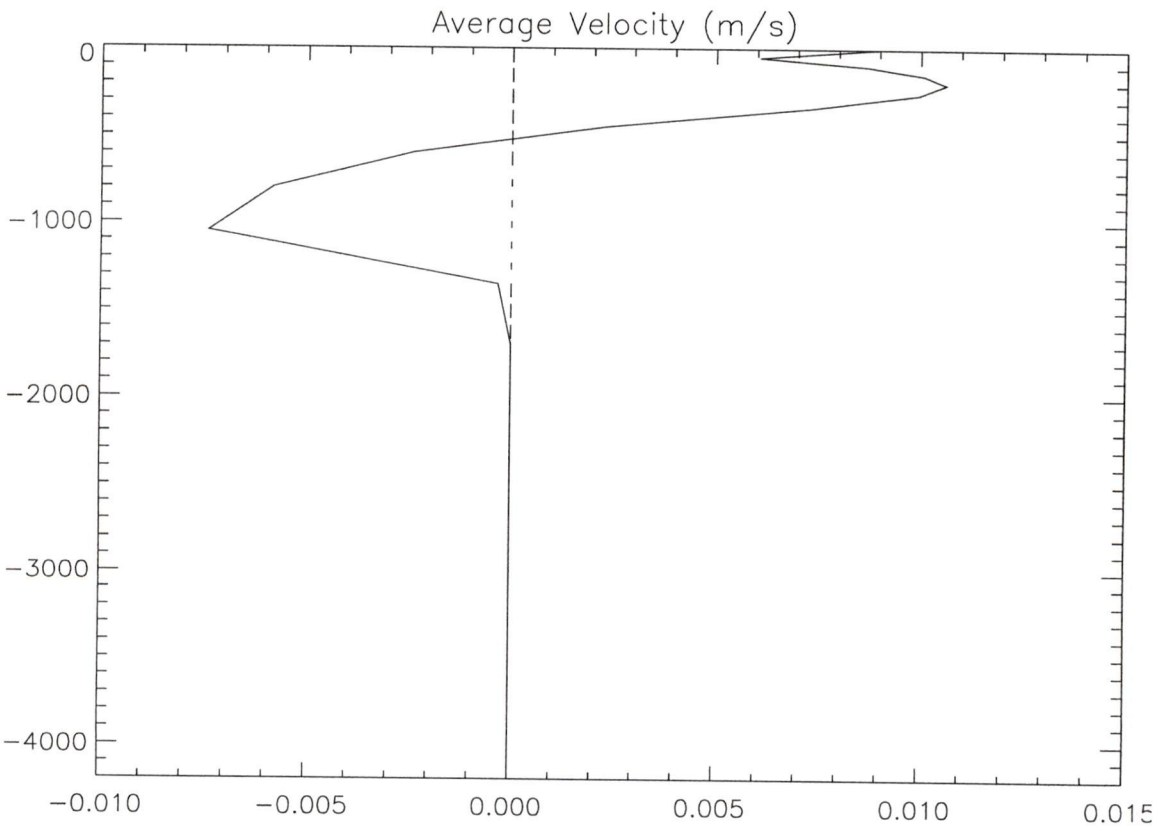

Figure 3.2.1: Vertical profile of flow through the Isthmus of Panama for mid-depth Isthmus (MIP). Positive indicates Pacific to Atlantic throughflow.

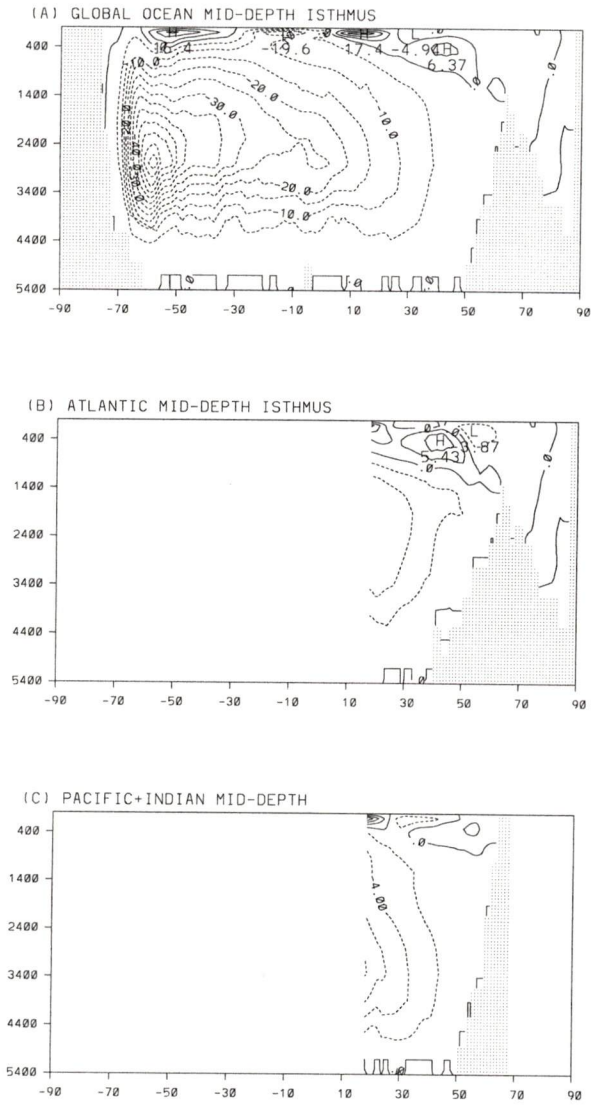

Figure 3.2.2: Meridional overturning streamfunction (in Sv = $10^6 m^3/s$) from the equilibrium climate in the case with mid-depth Isthmus (MIP) for (a) Global (b) Atlantic and (c) Pacific+Indian. The contour interval is 2 Sv in all cases and positive contours indicate clockwise circulation. Since it is only possible to define an overturning streamfunction in individual basins where there is land on both the eastern and western boundaries, the Atlantic and Pacific overturning plots are cut off at the Isthmus (b, c).

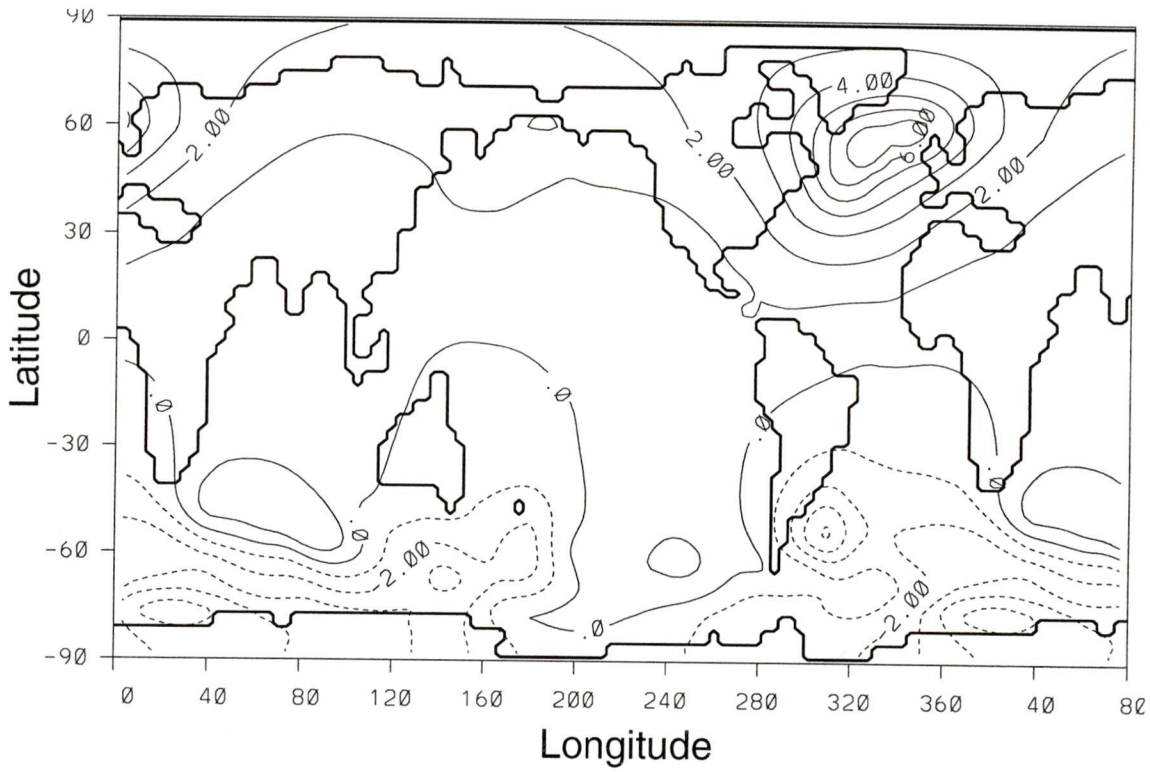

Figure 3.2.3 Global surface air temperature difference (°C) between the present day and mid-depth Isthmus (CTRL-MIP). The contour interval is 0.5 °C.

The transport through the sill for the SIP case is shown in Figure 3.2.4. The SIP net transport is also virtually 0 Sv with 0.5 Sv entering the Pacific from the Atlantic at the surface and 0.5 Sv returning just below it. With the shallow sill run (SIP) the North Atlantic SSS, and thermohaline circulation are only slightly different from CTRL. These results show that final model closure was most important in the tropical western Atlantic and eastern Pacific region, with only minor global effects (Figure 3.2.5).

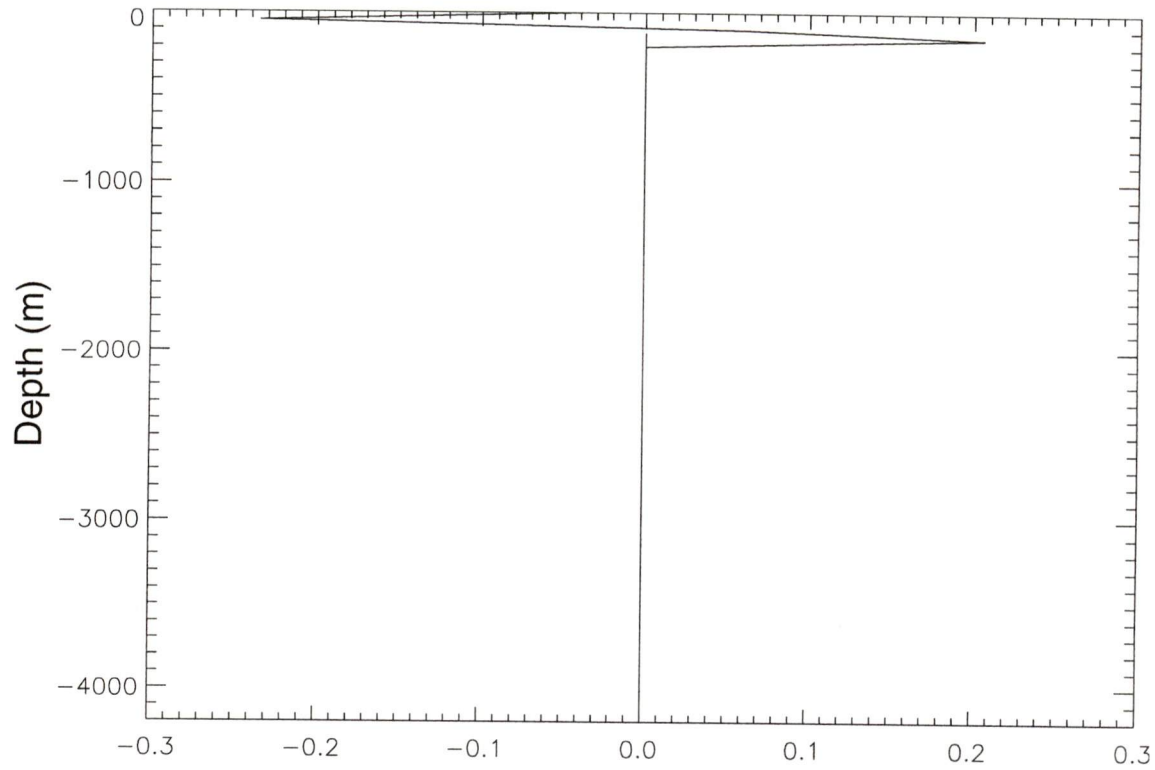

Figure 3.2.4: Vertical profile of flow through the Isthmus of Panama for shallow sill (SIP). Positive indicates Pacific to Atlantic throughflow.

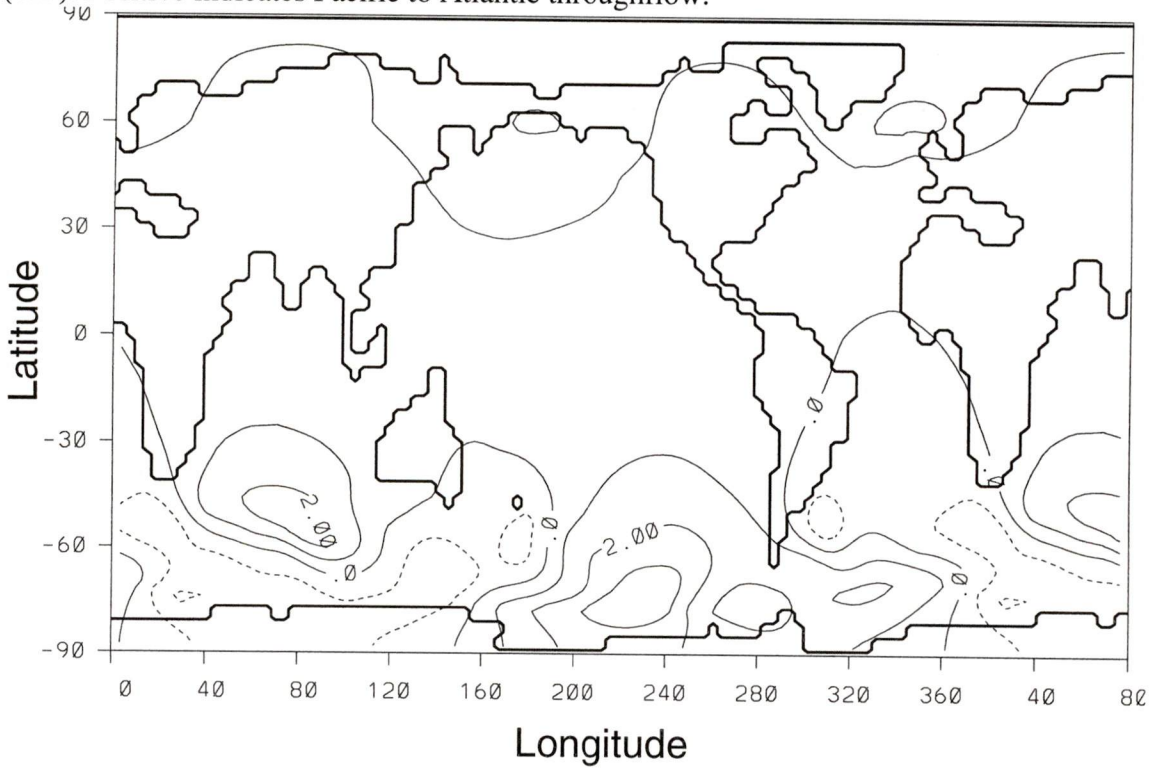

Figure 3.2.5 Global surface air temperature difference (°C) between the present day and shallow Isthmus runs (CTRL-SIP). The contour interval is 0.5 °C.

3.3 Effect of wind feedback (NWF)

The wind stress and wind speed feedback involves the calculation of the anomalous pressure field via the deviation of surface air temperature fields (from that of the control run), which are then converted into geostrophic wind vector anomalies, and finally a surface wind vector by rotation and contraction of the geostrophic wind vector. The result is an advective feedback mechanism on gyre, Ekman, sensible, and latent heat fluxes (see Fanning (1997) for more details on the wind feedback scheme used).

The wind feedback has been shown to be an improvement to model results (Fanning and Weaver, 1997a; Fanning, 1997), and hence it is incorporated into the perturbation runs. The anomalous wind stress vector for OIP is shown in Figure 3.3.1. The enhanced North Atlantic anticyclonic wind stress with the IP open would act to increase the Ekman transport of salinity anomaly out of the region. The increased wind speed also increased model latent and sensible heat transfer. These combined effects make the model less sensitive to the perturbation of opening the Isthmus.

An initial integration without the wind feedback in operation was performed (termed NWF), such that a comparison of NWF to OIP shows the effect on model results of the advective wind feedback. As expected from the combined effects of the wind stress and wind speed feedbacks as described above, notable differences between the salinity of NWF and OIP result. The direct effects on salinity also cause other minor differences between NWF and OIP thermohaline circulation, poleward heat transport and surface temperatures (e.g., Figure 3.3.2). Fanning (1997) showed that the presence of the wind feedback from the beginning of the integration or from later on in the integration made virtually no difference to the results.

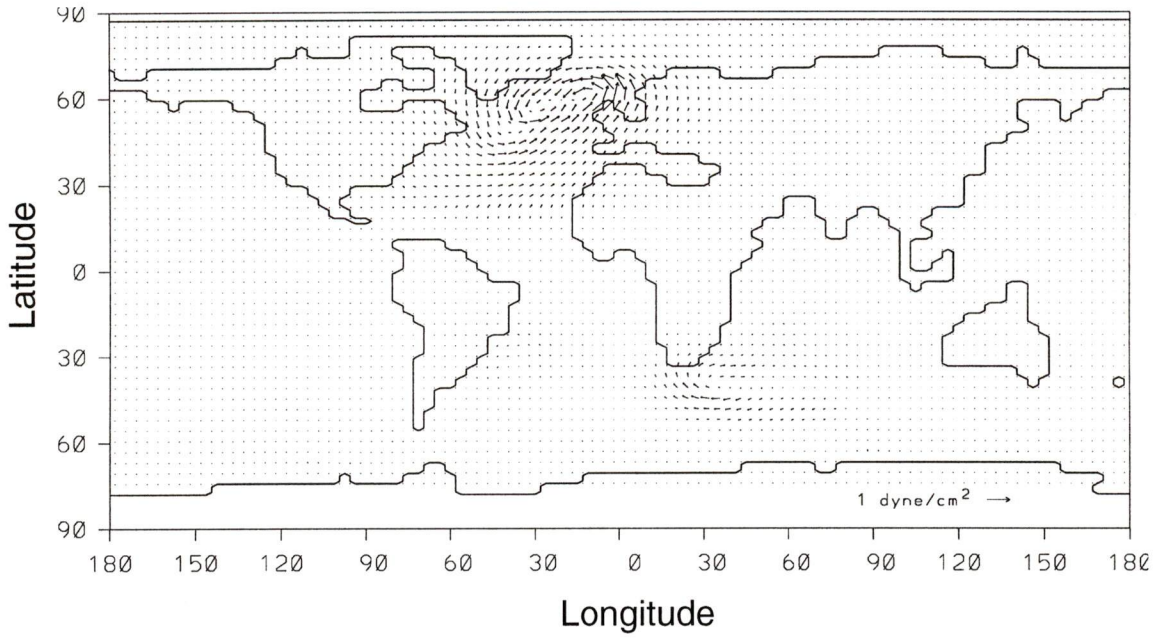

Figure 3.3.1 Anomalous wind stress vector (dynes/cm^2).

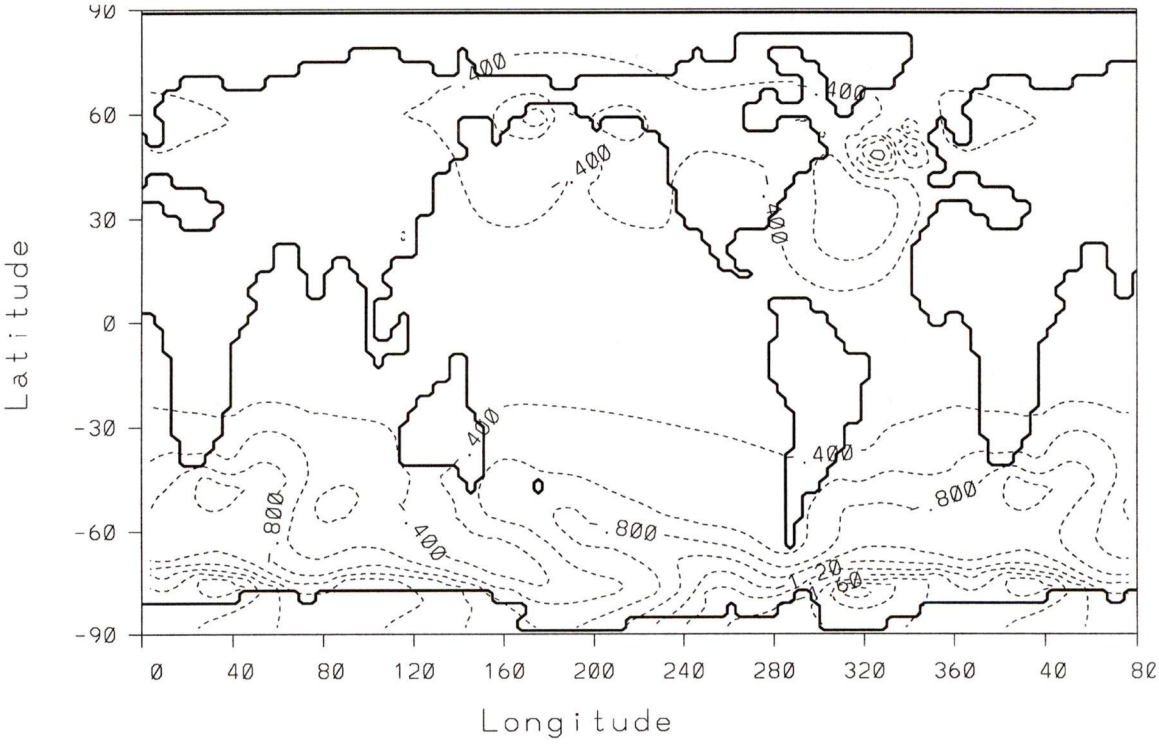

Figure 3.3.2: Temperature difference (°C) due to presence of wind stress feedback. Positive represents increased temperature with the wind feedback in operation. Contour interval is 1°C.

3.4 Greenland-Scotland ridge (CGS, CGSOIP)

Fluctuations in to Northern Component Water production (the precursor to NADW) have been related to changes in mantle plume activity of the Greenland-Scotland ridge over the past 25 Ma by Wright and Miller (1996). A sensitivity to the presence of the Greenland-Scotland ridge was performed by taking the extreme case—that with a complete ocean barrier all the way to the surface which spans from Greenland to Europe. (Hence, the Arctic is completely shut off from the rest of the world ocean as the Bering Strait is also closed in the model.) In this case, the prevention of fresh Arctic waters from entering the model North Atlantic causes an increase in NADW production (Figure 3.4.1 - albeit convection then only occurs south of the barrier).

This intensification of NADW upon Greenland-Scotland ridge closure is not consistent with Wright and Miller's (1996) assertion regarding the reduction of Northern Component Water upon increased mantle plume activity. However, the effect of complete isolation of the fresh Arctic in this run inhibits this result from refuting any link between Northern Component water and the Greenland-Scotland ridge mantle plume activity. A run to address this issue would require a representative sill depth (as planned by Mikolajewicz and Crowley, 1997). However, the result from these runs that an open IP drastically reduces NADW even with the intense NADW due to isolation of the Arctic, further supports the primary importance of the presence or absence of the IP with regards to NADW production, through its effects on North Atlantic SSS.

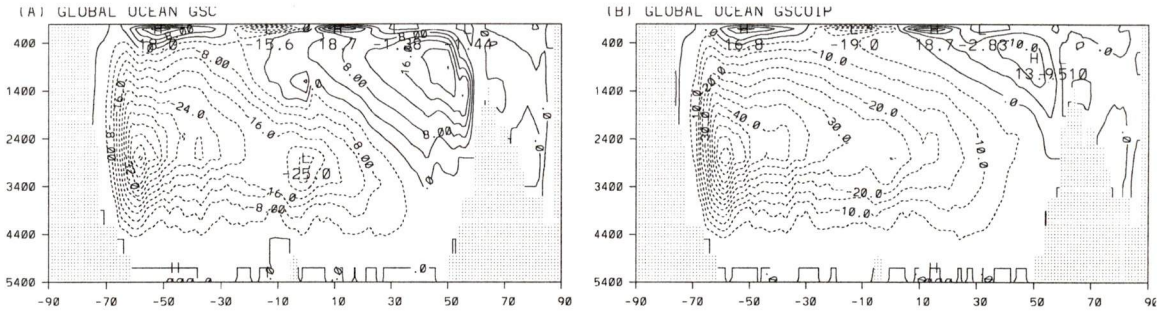

Figure 3.4.1: Global meridional overturning streamfunction (in Sv = $10^6 m^3/s$) from the equilibrium climate in the case with Greenland-Scotland Ridge Closed for (a) Isthmus also closed (GSC) (b) Isthmus open (GSCOIP). The contour interval is 2 Sv and positive contours indicate clockwise circulation.

4 Comparison to observations

Comparison of model results (§3) to observations from the biological and lithological record is necessary in order to assess the success of the numerical model's applicability to the current problem. Success also lends further confidence to the use of such models for future climate predictions (e.g., Gates *et al.*, 1995). Such data-model comparisons have been made where relevant in §3 above. Further intercomparison is made below, in order to address hypotheses based on observations alone. Keeping in mind the limitations and incompatibilities of model and data (§1.2), model results are compared to a wide variety of studies regarding the paleoclimate of the Late Neogene (Mid-Late Miocene and Pliocene), the time of IP closure.

The main form of deposition throughout the Mid-Late Miocene has been siliceous and carbonate oozes in the eastern Pacific and terrigenous material in the Caribbean. During this time, several deep-sea hiatuses occurred, associated with cool climates, low sea levels, and vigorous deep circulation (Keller and Barron, 1983). Sea level has been decreasing, with minor fluctuations since the Mid-Cretaceous, and was lower during the entire time of IP closure than it had ever been previously during the entire Phanerozoic (Hallam, 1977; Haq, 1984). Hence, lithological evidence of Cenozoic climate is rare on land, and most observations discussed below come from analyses of ocean cores. No attempt has been made to use a consistent time scale, as model results are compared to an extensive range of observations, and model runs are not simulations of any exact time periods (as discussed in §1.2).

4.1 Comparison to observations: regional

4.1.1 Carbonate and silica

Lyle *et al.* (1995) documented eastern tropical Pacific carbonate mass accumulation rates from 13 to 5 Ma by using reconstructions based on ODP and DSDP data. In the Late Miocene, ~10 Ma, there was a large drop in carbonate mass accumulation rates that occurred in the eastern Pacific. They discuss several other studies which have also shown evidence for the "carbonate crash" in the eastern equatorial Pacific. They address some explanations that have been proposed in the past and dismiss the possibility of a dramatic increase in primary productivity or sea level change as the cause. They propose that only two scenarios could have been responsible—one related to initiation of NADW production, and the other directly from changes in transport through the IP.

Lyle *et al.* (1995) calculated that changes in IP throughflow could have been responsible for the carbonate crash. Their calculation assumed Atlantic-Pacific throughflow, but the explanation may have still been feasible with Pacific-Atlantic throughflow. The model sill depth sensitivity results (§3.2) suggest that the net flow was either Pacific-Atlantic at this time, or near zero, with surface Pacific-Atlantic throughflow and Atlantic-Pacific return at depth (Figures 3.1.1 and 3.1.2). In any case, Lyle *et al.*'s (1995) explanation relied on the lack of observation of the carbonate crash in the Atlantic. Newer ODP results (Ocean Drilling Program, 1997) find the carbonate crash also in the Atlantic, ruling out this scenario.

Lyle *et al.* (1995) had also suggested a cause related to NADW initiation. Observations by Wright *et al.* (1992), based on isotopes from 41 ODP and DSDP sites worldwide suggest initial NADW intensification at 10.2-9.3 Ma. If the reorganization of flow caused by NADW initiation resulted in an increased import of more corrosive AABW, formed in the higher nutrient Antarctic, into the eastern Pacific upon NADW initiation, it could have caused the carbonate crash there. They did not expect to find such a

carbonate crash in the Atlantic, but they had assumed Atlantic-Pacific throughflow. The equatorial Atlantic could have also been affected by AABW being imported to the eastern Pacific and then flowing through the open IP. Indeed, this could explain why the carbonate crash lasted 1.0-1.5 Ma longer in the Pacific than in the Atlantic. They abandoned this scenario because of inadequate faunal and isotope evidence to address increased AABW into the Pacific. Model results shown in Figure 3.1.3 displays that AABW production was indeed intensified for the Pacific (Figures 3.1.3 e, f). Modelled velocities at depth (not shown) suggest that intensification of North Equatorial Current (NEC) export of eastern tropical Pacific water upon closure could possibly also have been a factor.

Subsequently, Caribbean carbonate concentrations were ~ 20% lower than Pacific values, gradually increasing from 6.2-3.8 Ma, at which time values were similar. The gradual increase in Caribbean carbonate was attributed by Keller *et al.* (1989) to a decrease in old, corrosive AABW into the region, and a increase in NADW. McDougall (1996) also interprets benthic foraminiferal observations as indicative of a change from AABW to NADW in the Caribbean and Pacific Deep Water (PDW) in the eastern equatorial Pacific, occurring after ~6.7 Ma.

Silica deposition occurred on both sides of the IP until ~ 10 Ma (Keller and Barron, 1983). Silica accumulation is associated with less vigourous circulation (older, deep waters). MM noted that initial NADW production associated with IP closure could have been responsible for the sudden cessation of silica deposition in the Caribbean ~ 10 Ma. Here it is also noted that a potential change from Pacific-Atlantic throughflow at depth to an Atlantic-Pacific throughflow (§3.2) could have also played a role in this transition.

4.1.2 Temperature and nutrients

Diachronous radiolarian speciations and extinctions in the eastern equatorial Pacific have been studied by Moore *et al.* (1993). They show patterns indicative of shifts in the

areas of high productivity over the past 10 Ma. A southward shift of the South Equatorial Current (SEC) was shown ~7-6 Ma, possibly related to gradual Northern Hemisphere cooling. They also found evidence for a slight northward shift of the SEC ~3.7-3.4 Ma, which is postulated to be due to IP closure. Model resolution is too coarse to compare to these hypotheses.

However, radiolarian events in the same region have also been interpreted as evidence for a general cooling trend in the Miocene (Moore and Lombardi, 1981), which was attributed by the authors to a gradual reduction in IP throughflow. Indeed, colder Pacific water which had been exiting into the model Atlantic was diverted back into the Pacific upon IP closure. Hays *et al.* (1989) find no such cooling trend for DSDP sites 572 and 573 between 3.7-2.4 Ma, however. They suggest two explanations: that the cooling was not present at their location or that it was not present at 3.7-2.4 Ma because the temperature change was a result of the closure to deep water. Analysis of model results from the deep and shallow sill runs lends support to the second scenario. Figure 4.1.1 illustrates the effect on temperature at 125m (where radiolarians are most abundant—Kling, 1978) of the entire IP closure, and shows a cooling in the tropical eastern Pacific. Figure 4.1.1a shows that the shallow sill run and present day run are not significantly different in this area—thus the difference seen in Figure 4.1.1b is entirely due to the closure to deep water, and hence observed in radiolarian bioevents of the Miocene but not the Pliocene. Keller *et al.* (1989) also note Pacific bottom water cooling relative to the Caribbean at 6.2 Ma from foraminiferal data.

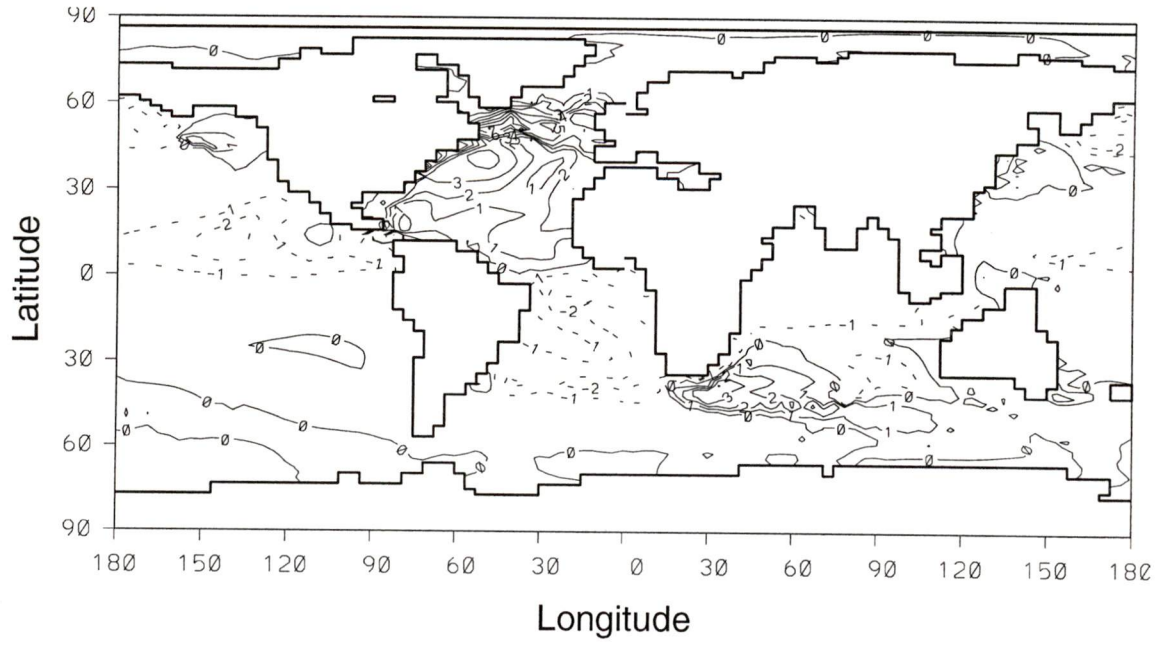

Figure 4.1.1: Temperature change at 125 m (maximum radiolarian abundance) for entire effects of Isthmus closure (over > 12.5 Ma) (CTRL-OIP). Negative indicates cooling as the Isthmus closed.

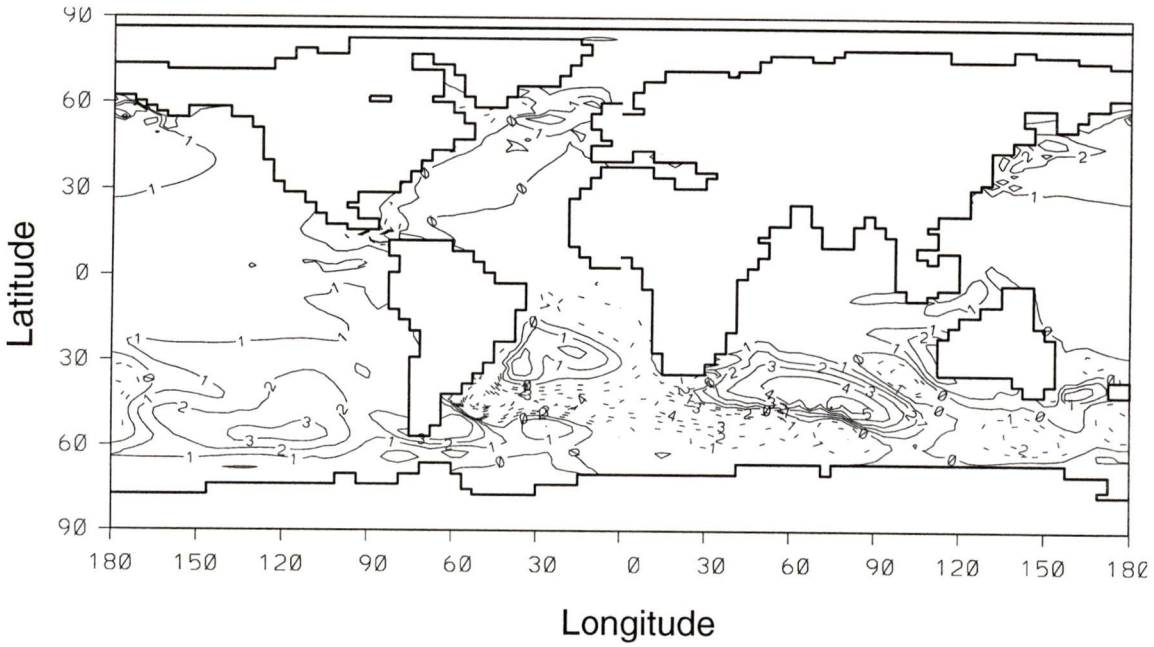

Figure 4.1.2: Temperature change at 125 m (maximum radiolarian abundance) for effects of shallow closure only (representative of difference from ~4 Ma to today) (CTRL-SIP). Negative indicates cooling as the Isthmus closed.

4.1.3 Upwelling

Keller *et al.* (1989) performed an analysis of planktonic foraminifera from DSDP holes in the Caribbean and East Pacific. They found increases in Caribbean populations which thrived in upwelling currents between 6.2 to 3.2 Ma. In addition, Pujos (1987) analyzed calcareous nannofossil sediment records in the eastern tropical Pacific and determined that as the IP closed, the Peru-Chile current strengthened and more upwelling occurred around the Galapagos Islands. Model upwelling results in this region (not shown) do not compare favourably with these observations, even when considering mid and shallow depth runs. This is not strong enough evidence to dismiss IP closure as the cause of the upwelling in this region, as open-ocean upwelling is largely dependent on ocean-atmosphere interactions neglected by the simple atmosphere of the model (FW).

Houghton (1989) also found nannofossil biostratigraphy evidence for increased upwelling in this region during the Late Pliocene, and suggested it may have been due to westward diversion of Pacific water upon IP closure. Model results are not inconsistent with this scenario: there was an intensification of the westward NEC as the Pacific-Atlantic throughflow was blocked.

Sancetta (1983) determined that the latest Miocene was a time of high productivity for calcareous and siliceous organisms, also suggestive of a major upwelling of the Peru-Chile current, which is ultimately derived from AAIW. Model results concur with increased AAIW production (Figure 3.1.3) and increased upwelling of this current (not shown). She found low productivity in the open ocean (Site 503, ~1000 miles west of the coast) tropical Pacific during the Pliocene, and high productivity near the coast (Sites 504/505) until ~3 Ma. While the model cannot address the open ocean result, it does seem to support a more vigorous upwelling (and hence nutrients) in the region until ~3 Ma (greater upwelling in the deep and mid-depth runs, but not the shallow run - not shown).

Weaver (1990) speculated that prior to IP closure, the California Current may have been much weaker, if not reversed, through analogy with the Leeuwin Current off Western Australia. This would have caused a milder and wetter climate along Baja and California when the IP was open. Model resolution is too coarse to resolve this eastern boundary current and hence to verify or reject this speculation. However, there are results consistent with it: the thermocline along the coast of both North and South America warmed and the steric height difference (relative to 1000 m) between the Isthmus (14°N) and off California (42°N) increased by 11 cm when the IP was opened. Furthermore, upwelling along the North American west coast was suppressed, as Weaver (1990) suggested (not shown), which would have meant a decrease in primary productivity there.

Allmon *et al.* (1996) examined extensive Pliocene paleontological evidence off Florida. They suggested that direct changes to currents and upwelling in the area due to the IP rise, as well as indirect effects through NADW formation (which results in a net nutrient transfer to the Pacific) would have been important. They proposed that Weaver's (1990) analogy would have meant upwelling of nutrients occurred along the east coast of Florida with the IP open, but not after closure. Indeed, they found evidence for decreased biological productivity in the region at ~3.5-2.5 Ma, coincident with the time of final closure. Again, model resolution is not appropriate for comparison in this case. They also noted that some biological changes in the area can be found that can not be related to the IP rising and closing, and may instead be due to other factors such as changes in average global conditions.

4.1.4 Evolution

IP closure provides an opportunity to test the fundamental biological question as to the extent to which biota are affected by geographical isolation and environmental change. Initial analyses (e.g., Vermeij and Petuch, 1986) found evidence for a mass extinction ~3

Ma of American molluscs which was more severe in the western tropical Atlantic (32%) than the eastern tropical Pacific (15%). The difference was partly due to the Atlantic's higher degree of endemic faunas as endemic taxa had extinction rates of over 50%. These initial data were also influenced by sampling bias (far more records in the Pacific).

Allmon *et al.* (1993) found that ~2.4 Ma, 70% of western tropical Atlantic mollusc species became extinct, compared to 30% in the eastern tropical Pacific. Contrary to earlier results, overall regional diversity has not changed since 4 Ma in the tropical Pacific or Atlantic. Allmon *et al.* (1996) and Jackson *et al.* (1993) show that IP closure in fact triggered a 40% increased Caribbean diversity, which was balanced by extinctions at ~1.5 Ma. Since the temperate Atlantic did not experience this increased diversity from IP closure, but did suffer from the extinctions at ~1.5 Ma, diversity is today only a fraction of its Pliocene value there (e.g., 40% off Virginia).

Barnes *et al.* (1995) include these western Atlantic molluscan extinctions in an outline of global stratigraphic bioevents. They consider the extinctions to be two phases of the Early/Late Pliocene bioevent. They note that sea-level drop and cooling occurred at these times. The relative importance of these effects to the effects of increased western Atlantic salinity and changes in water mass types due to IP closure is not clear. The cooling trend superimposed on the paleoclimate during IP closure is addressed further in §4.2.1.

Changes in global oceanic salinities, temperatures, and water masses had evolutionary effects on marine biota. These effects will not be addressed individually here. Instead, they are referred to only when such effects allow interpretation of some paleoclimatic effect, and as such are referred to throughout the thesis. Two examples include adaptation of snapping shrimp to more saline conditions in the Caribbean which help constrain timing of IP closure (§1.1) and are in agreement with a gradual increase in Caribbean salinity from ~4-2 Ma (§3.1), and evolution of radiolarians due to changes in

water masses (Kling, 1978) which suggest effects on eastern Pacific upwelling and temperatures (§4.1.2).

4.1.5 ENSO

Thermocline depth along the equatorial Pacific is an important element to the El-Niño/Southern Oscillation (ENSO). There are significant differences between modelled open and closed IP thermocline (not shown). If the frequency, magnitude, or pattern of ENSO events was different with an open IP, could this be linked to any bioevents? Could the change from a previous mode to the modern one upon IP closure be linked to any bioevents? Vermeij (1989) has examined the possibility of a role of ENSO itself on evolution, but did not consider whether a change in the character of ENSO has occurred in the past and what potential effects this could have had.

The numerical model does not have adequate resolution nor the necessary atmospheric dynamics to directly address how ENSO may have been different with an open IP. Ongoing studies on the impact of global warming on ENSO at institutions worldwide may provide some suggestion as to precisely how ENSO would have behaved, if present at all, with an open IP. At present, such studies are only preliminary but do at least show that changes can be expected in the character of ENSO under different climates (Knutson *et al.*, 1997). Thus it is conceivable that IP closure could be linked to bioevents resulting from changes in the character of ENSO, which warrants investigation of the fossil record with this possibility in mind.

4.2 Comparison to observations: global

4.2.1 NADW production

Evidence of initial forms of NADW production (Northern Component Water) have been observed as early as ~ 30 Ma (sediment redistribution: Miller and Tucholke, 1983; carbon isotope records: Miller and Fairbanks, 1985). However, NCW has been

more common since ~13 Ma, coincident with initial closure and the subsidence of the Iceland-Faroe ridge (Blanc *et al.*, 1980). Evidence for an increased NADW production ~ 10 Ma (well after Iceland-Faroe ridge subsidence, but coincident with initial IP closure) includes benthic foraminiferal carbon and oxygen isotopic and faunal abundances (Woodruff and Savin, 1989), as well as the silica and carbonate observations discussed above (§4.1.1). Model results are also consistent with this scenario (c.f. Figures 3.1.3 and 3.2.2). NADW similar to present-day has only been in operation since ~2.5 Ma, coincident with final closure (Wright *et al.*, 1991, 1992) and also consistent with model results (Figure 3.1.3). These results suggest that although presence or absence of the IP is not the only factor governing NADW production, it is the main one. The scenario is one in which, upon closure, the climate of the North Atlantic was more conducive to NADW production due to increasing North Atlantic SSS. Perturbations to NADW formation were forced by changes in orbital forcing, CO_2 levels, tectonics of the Greenland-Scotland ridge and other forcing factors via interactions and feedbacks within the climate system (e.g., Kutzbach, 1992; Wright and Miller, 1996). This proposed scenario is consistent with a model study of restriction of flow through the IP (Mikolajewicz and Crowley, 1997).

The meridional overturning for CTRL and OIP is illustrated in Figure 3.1.3 for the Global, Atlantic, and Pacific+Indian basins. As discussed in FW, the ocean climatology in the coupled model is comparable to similar ocean-only simulations with 19 Sv of deep water forming in the North Atlantic, about 12 Sv of which is exported into the Southern Ocean. The deep Atlantic and Pacific Oceans are filled with Antarctic Bottom Water (AABW) originating in the Weddell and Ross Seas. The equilibrium state of the atmosphere in the coupled model (not shown) also compares favourably with observations (see FW for details). The most striking feature in Figure 3.1.3 is the complete absence of NADW with an open IP. In fact, the overturning in the Atlantic resembles both the Pacific

Ocean overturning of the CTRL and OIP runs, with the deep basin waters originating from the southern hemisphere. Associated with the lack of NADW prior to IP closure is a reduction in oceanic heat transport (both global and Atlantic – Figure 3.1.4a; Table 3.1.1), resulting in colder North Atlantic surface air temperatures (Figure 3.1.5). In the Pacific, however, the oceanic heat transport actually increased slightly although it still remained partitioned nearly equally between the vertical-meridional and horizontal components. Figures 3.1.3a and b also show that with the Isthmus open, slightly more AABW and Antarctic Intermediate Water production occurs.

4.2.2 Poleward heat transport

Modelled poleward heat transport is compared to observational estimates at 24°N (Bryden, 1993). This value is chosen because warm western boundary currents in both the Atlantic and Pacific basins make this latitude close to that of maximum transport and the Indian Ocean can be neglected at this latitude. It is a good location for comparison with the model as the modelled E-P (and hence Q_{LW}) compares better with observational estimates in this region than most others and the heat transport does not vary much with latitude around 24°N. Figure 3.1.4 shows the oceanic poleward heat transports. The CTRL oceanic heat transport reaches a maximum of about 1.1 PW in the northern hemisphere, with slightly larger southward heat transport in the southern hemisphere. Direct observations at 24°N (Bryden, 1993 — Table 3.1.1) suggest that the global ocean transport is closer to 2 PW at this latitude. The weak ocean heat transport in our model is typical of that found in coarse resolution OGCMs. Nevertheless, when normalized by the total global heat transport in the model, the mechanisms for heat transport in the global ocean and in the individual basins are similar to observations at 24°N (Table 3.1.1). Specifically, both in the observations and in the model about 2/3 of the total ocean heat transport at 24°N is accomplished through the meridional overturning in the Atlantic. The remaining 1/3 comes

from the Pacific Ocean where it is equally partitioned between the vertical-meridional and the horizontal components. This agreement between model results and observations in the present-day climate gives us confidence in our paleoclimatic sensitivity analysis discussed below.

The reason for the decreased heat transport in the Atlantic and increased heat transport in the Pacific Ocean is as follows: with an open IP, there is no longer a land boundary to allow an east-west pressure gradient and hence northward geostrophic flow to develop. Thus warm, saline South Atlantic waters which today travel in a western boundary current into the North Atlantic, remain in the South Atlantic (or head southwards) creating a slightly warmer climate there (Figure 3.1.5). In addition, relatively cold, fresh Pacific waters flow through the IP into the Atlantic over the entire water column, with a total transport of 15.6 Sv. This Pacific-to-Atlantic throughflow eventually exits the South Atlantic into the Southern Ocean. The result is a weaker, fresher and cooler Gulf Stream in the Atlantic, and a slightly warmer Pacific Ocean. The Gulf Stream thereby advects less salt northward and so precipitation and runoff dominate the freshwater budget, making the high North Atlantic water too fresh to convect.

The vertical-meridional component (Ekman plus vertical overturning) of the total oceanic heat transport in a given basin (Table 3.1.1) is approximately given by $Q_{VM} \propto V\Delta T$, where V is a depth-averaged northward transport in the thermocline and ΔT is representative of the temperature difference between the thermocline and subthermocline waters. The decrease in Q_{VM} in the Atlantic Ocean prior to IP closure is therefore directly attributed to a substantial reduction in V due to the absence of NADW formation, whereas in the Pacific Ocean, the slight increase in Q_{VM} is associated with a slight increase in ΔT.

The decrease in ocean heat transport prior to IP closure is largely compensated for by an increase in atmospheric heat transport. Hence, the total planetary heat transport

remains largely unchanged. The OIP run has slightly colder high latitudes (on the zonal average), thus a slightly greater equator-to-pole surface air temperature gradient and hence sensible heat transport. While the latent heat transport did not change much at high latitudes, it did increase slightly near the subtropics of the northern hemisphere due to the warming of the Pacific Ocean which dominates the zonal mean at these latitudes.

This comparison has focused solely on the OIP and CTRL runs so far. From Table 3.1.1, it can be noted that the shallow run (SIP) is similar to observations and the model Isthmus closed (CTRL) run in the Atlantic. However, the Pacific results are quite different. In order to understand this, consider first the mid-depth run Atlantic results. The second column of Table 3.1.1 shows that as the Isthmus opening becomes wider from CTRL to SIP to OIP , the vertical component of the thermohaline circulation is reduced in each case. One might expect the mid-depth MIP run to fall between SIP and OIP. Instead, the poleward heat transport is split equally between the two components. In this case, however, it is not suitable for an analogy to the present-day Pacific, because the thermohaline circulation is still fairly active in this run (Figure 3.2.2). The explanation for the difference has to do with the major change to the nature of the throughflow between MIP and OIP, as noted in §3.2. There is less cold Pacific water entering the Atlantic in MIP than in OIP (Figure 3.2.1). Figure 4.2.1 shows the difference in model Atlantic temperatures between OIP and MIP. This figure shows that the MIP model Atlantic was slightly cooler at the surface and up to 3°C warmer at depth. Returning to the analogy of vertical-meridional poleward heat transport $Q_{VM} \propto V\Delta T$ as defined above, ΔT and hence Q_{VM} in MIP would be significantly reduced. The barotropic component, however, is not much different as the thermocline waters between the two runs are not much different.

The Pacific meridional transect difference plot (Figure 4.2.2) shows that the MIP Pacific was generally warmer than OIP everywhere. In fact, MIP warming is even larger at

depth than in the thermocline. Hence, ΔT and thus Q_{VM} would be expected to be reduced. Indeed, Q_{VM} is reduced to such a degree that it is practically zero. The barotropic heat transport increased somewhat however, due to the increased thermocline temperatures. The shallow Isthmus (SIP) Pacific behaves similarly to the MIP Pacific, with the difference between MIP and SIP Atlantic owing to the intense thermohaline circulation (near that of CTRL) and hence higher V, in SIP.

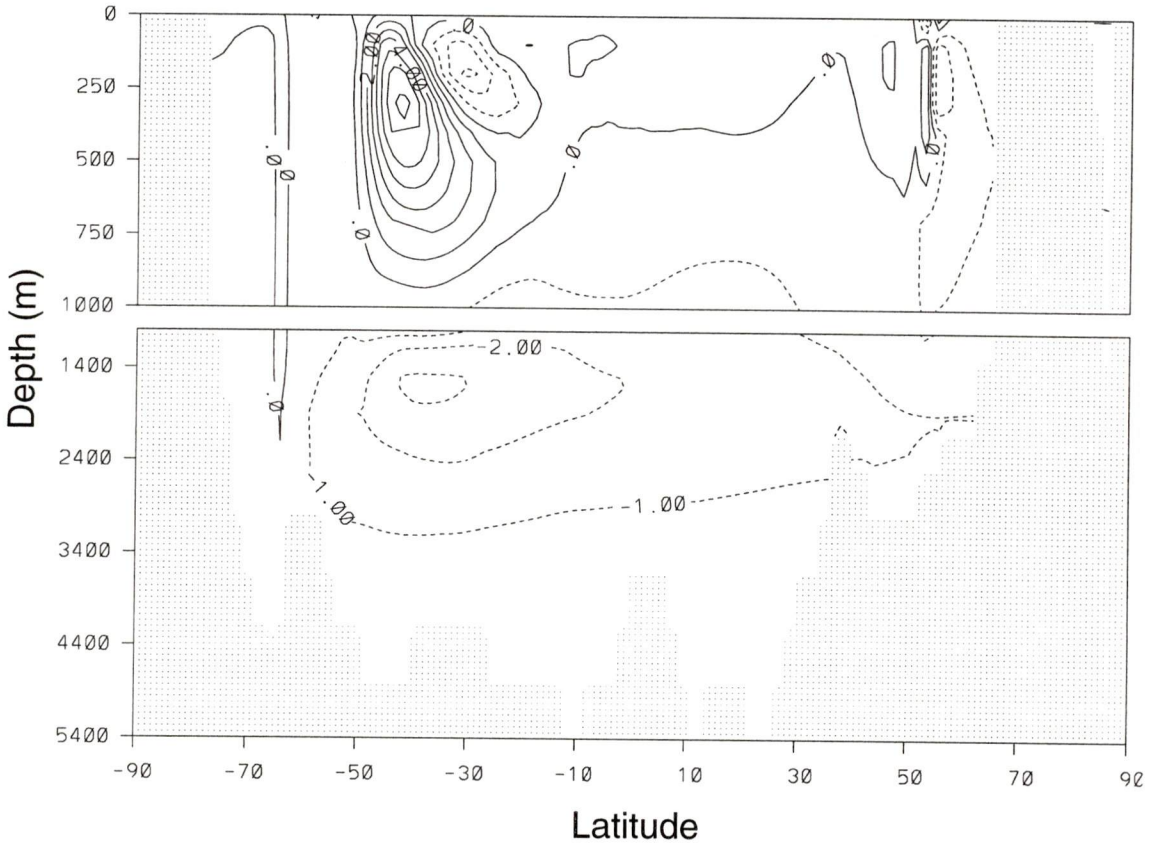

Figure 4.2.1: Atlantic vertical temperature profile difference (°C) between mid-depth Isthmus and deep open Isthmus runs (OIP-MIP). Contour interval is 1°C. Positive indicates OIP warmer than MIP.

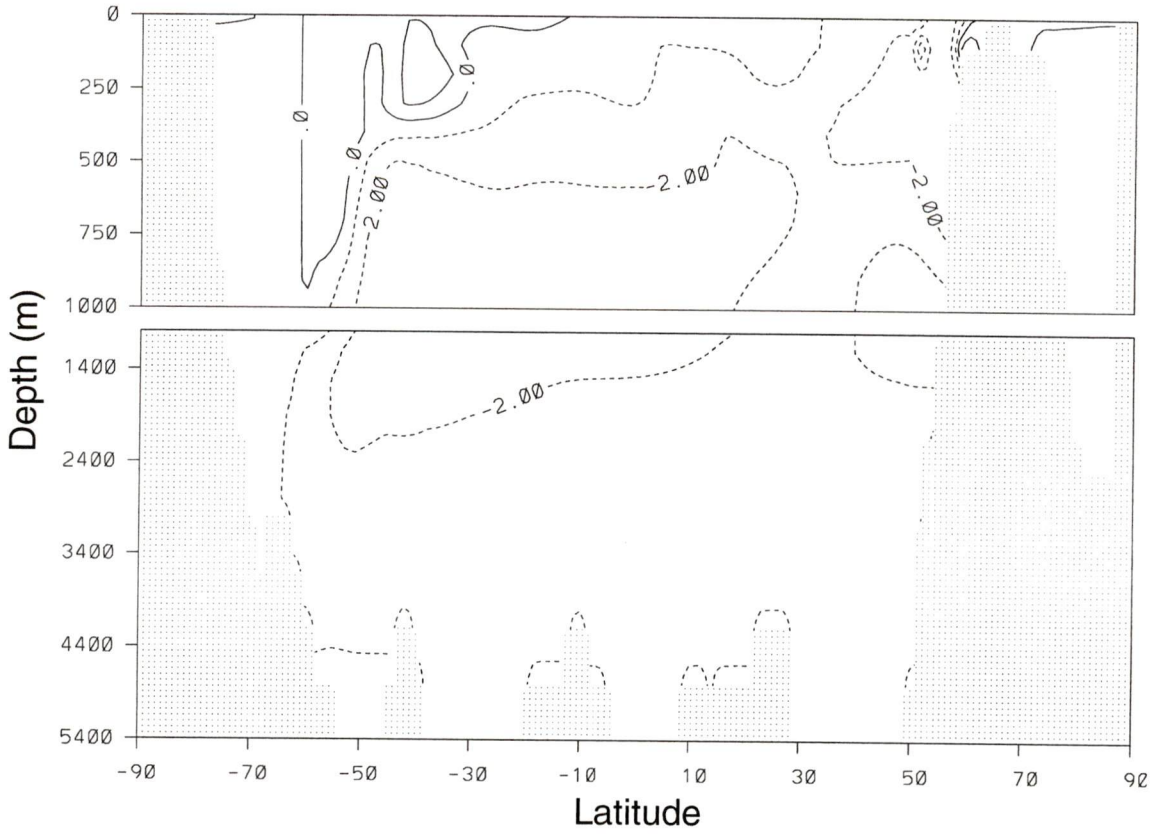

Figure 4.2.2: Pacific vertical temperature profile difference (°C) between mid-depth Isthmus and deep open Isthmus runs (OIP-MIP). Contour interval is 1°C. Positive indicates OIP warmer than MIP.

4.2.3 Temperature

The comparison of model runs to global temperature patterns is made difficult because of the slow closure of the IP. During the closure, the climate of the real world was affected by the gradual Cenozoic cooling trend (e.g., Kennett, 1982; Crowley and North, 1991). This trend can be attributed at least in part to the long term oscillations proposed by Fischer (1982). The fluctuations in NADW production, themselves seemingly governed by IP closure (§4.2.1), would have been an important factor to global temperature as they occurred. The modelled warming due to IP closure may thus be partly responsible for the warm period ~ 3 Ma (e.g., Dowsett *et al.*, 1996). The sensitivity results mean then that if the IP had not closed but Northern Hemisphere glaciation had been able to occur, the North Atlantic would now be several degrees cooler than it is today.

Expected but undocumented warming throughout the Miocene and Pliocene could have offset expected but undocumented cooling during this time from other factors such as drawdown of CO_2 by more intense weathering due to uplift of the Tibetan plateau and North American west (e.g., Burbank, 1992; Filippelli, 1997). Some other important factors affecting global temperatures during the time of IP closure include passive margin uplift around the North Atlantic (Eyles, 1996), Miocene vegetation changes (Dutton and Barron, 1997) and North Pacific volcanism (Rea *et al.*, 1995).

4.2.4 Northern Hemisphere glaciation

Is it plausible that IP closure could have been the forcing responsible for the Late Pliocene initiation of Northern Hemisphere glaciation? If so, how can the increased temperature due to intensified poleward heat transport be reconciled with observations of decreased temperatures and glaciation at this time (Kennett, 1982; Berggren, 1982; Crowley and North, 1991)? Recent fossil discoveries (Svitil, 1996; Gore, 1997) have led to the hypothesis that important steps in the early evolution of humans were related to the paleoclimatic effects in Africa of the initiation of Northern Hemisphere glaciation at the Late Pliocene event ~3 Ma.

Stanley (1996) hypothesized that the coincident timing of closure and Northern Hemisphere glaciation could be linked via the following mechanism: Prior to NADW initiation, the Gulf Stream had flowed into the Arctic bringing an enhanced poleward heat transport to the region. After closure sinking (NADW initiation) reduced the northern extent of the Gulf Stream and its poleward heat transport. There is no model support for this mechanism. Furthermore, it suffers from conceptual difficulties as well. The Gulf Stream was weaker and not as warm prior to IP closure, so even if there were model support for increased transport to the high North Atlantic prior to IP closure, it may not have transported a significant amount of heat. Model circulation (not shown) suggests

instead that the Gulf Stream waters advected northward simply returned as part of the barotropic gyre with the IP open (as may be expected).

Berggren (1982) argued that upon IP closure, increased amounts of warm subtropical waters would have moved northward in the Atlantic and that this stronger and warmer Gulf Stream could have lead to intensified evaporation at midlatitudes and hence precipitation over eastern Canada, Greenland and Western Europe, providing the moisture required for glaciation. Ruddiman *et al.* (1980) have also suggested that an intensified, warmer Gulf Stream could have contributed to conditions favorable to ice sheet growth by causing a vigorous meridional atmospheric circulation associated with a strong temperature gradient at the eastern coast of North America.

The model North Atlantic did warm significantly upon IP closure (Figure 3.1.5) due to NADW initiation. Associated with the warmer North Atlantic was increased evaporation and precipitation along its borders. Area-averaged model evaporation increased by approximately 1.0 cm/yr from 23°N-49°N and precipitation increased by 0.4 cm/yr from 49°N-88°N. Surface specific humidity (Figure 4.2.1) is consistent with North America becoming wetter upon IP closure. These results are also consistent with evidence for North America being driest ~7-4 Ma (wind blown eolian deposits of DSDP cores: Axelrod and Raven, 1985; Late Miocene expansion of range of grazing animals: Repenning, 1967).

Although these results are consistent with Berggren's (1982) hypothesis it is not possible to completely refute or verify it on the basis of model output (model E is highly parameterized and specific humidity is only a proxy for precipitation). A more sophisticated analysis of the problem should use a model including the following, listed in order of most to least important: an appropriate land ice scheme, Milankovitch orbital forcing, a seasonal cycle (which is important for development of ice cover during the cold

winter), atmospheric dynamics and additional physics, including a more realistic hydrological cycle. Finally, it would also be useful to consider the role of an open Bering Strait (Wijffels *et al.*, 1992; Reason and Power, 1994). The next suggested step of incorporating an ice sheet model (Marshall, 1997) is currently in progress.

Evidence (§1.1) points to intermittent final closure of the IP around the time of Northern Hemisphere glaciation. If this was the case, oscillations between shallow and closed IP could have brought the moisture needed during the closed phase, and brought some cooling during a shallow opening phase. In this case, NADW reduction could have also played a role in the cooling event associated with initial Northern Hemisphere glaciation ~2.9 Ma via poleward heat transport as well as carbon uptake changes. If so, it would have worked together with one or more other mechanisms which have been proposed to explain Northern Hemisphere glaciation in the past such as orbital cycles (Cronin *et al.,* 1996) and cooling around the time of Northern Hemisphere glaciation (as discussed in §4.2.3).

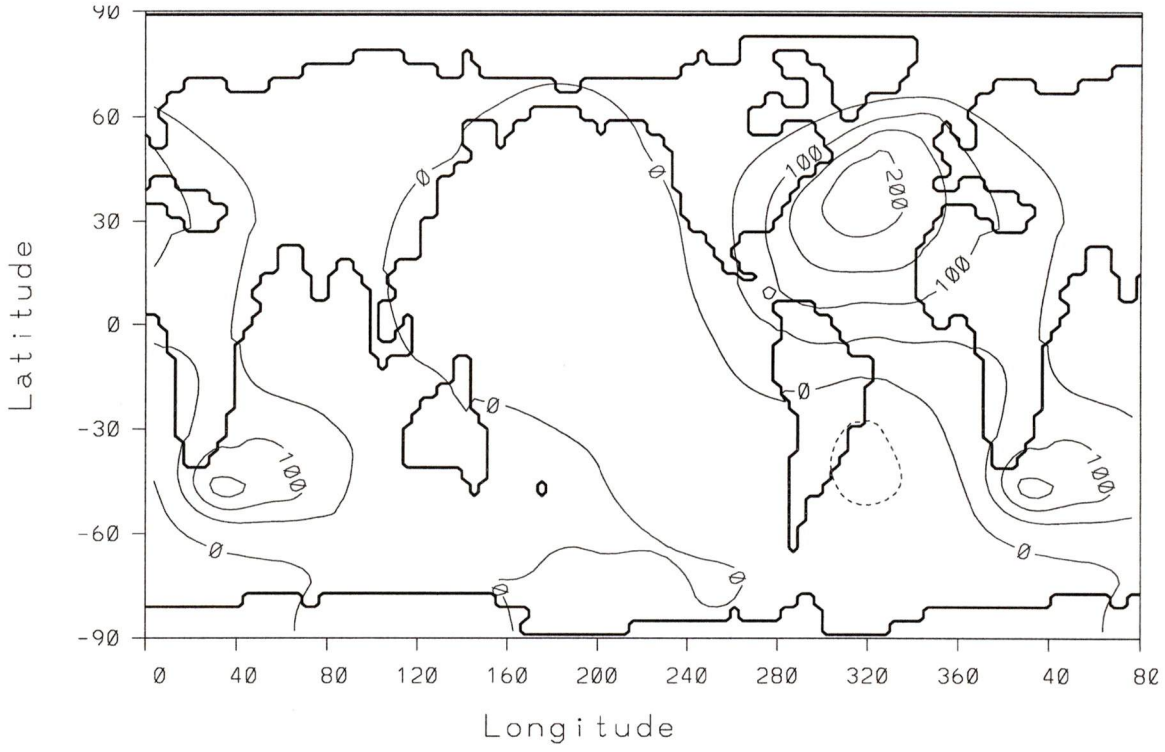

Figure 4.2.3: Change in surface specific humidity (g/kg) (CTRL-OIP). Positive indicates more moisture content as the Isthmus closed (dryer when the Isthmus was open).

5 Summary and Conclusions

This study is not an attempt to reconstruct the detailed history of Late Miocene/Pliocene paleoclimate. Rather, it is a perturbation analysis focused on the mean-climatic changes one might expect between regimes with an open IP and with it closed. Model limitations, such as coarse resolution as well as various parameterizations and assumptions, must be kept in mind when analyzing results. It is also noted that the model incorporates only the major perturbation of the IP closure, and hence eliminates the possibility of modelling any result which depended on a combination of events. However, a synthesis of observational studies with model results allows for a deeper understanding of scenarios than conclusions based on one study alone. Model results prove particularly useful in addressing proposed mechanisms from observational studies and highlighting areas requiring additional study, as outlined in the conclusions below.

The closure of the Isthmus of Panama (IP) has been shown to have significant effects on Late Miocene and Pliocene paleoclimate. These range from regional changes such as upwelling of nutrients and effects on evolution to global effects through deepwater changes (initiation of NADW production) and associated increased poleward heat transport. The agreement between several observations and model results discussed above lends support to both the use of the climate model under different climatic forcing, as well as to the importance of paleogeography as a climatic and biological forcing factor. Several conclusions can be made based on model-data intercomparison, including:

1. Determination of the direction of IP throughflow is complicated. Several studies assume net throughflow in both the Atlantic-Pacific and Pacific-Atlantic directions. Pacific-Atlantic flow is modelled with the deep sill (OIP). As the model sill rose, deep Atlantic-Pacific exchange did occur, but with no net Atlantic-Pacific throughflow. It is

unclear whether model sill depths could exist which would result in net Atlantic-Pacific throughflow. However, observations (Collins *et al.*, 1997) are also consistent with net Pacific-Atlantic throughflow. Usually the important factor is Pacific and Atlantic water property homogenization, so this point is irrelevant. In some cases (e.g., Mullins and Neumann, 1979; Lyle *et al.*, 1993), a particular direction is required.

2. Miami terrace submarine erosion had been interpreted to imply IP closure by the Mid-Miocene (Mullins and Neumann, 1979). This conclusion was based on the assumption of Atlantic-Pacific throughflow. Subsequent work has shown that the IP was open until the Late Pliocene, suggesting that the observations were (i) not related to IP closure, (ii) responding to the cutoff from deep water, or (iii) evidence that the IP was closed at this time, but reopened later.
3. Once the IP closed, the climate of the North Atlantic was more conducive to NADW production. Perturbations to NADW formation then most likely arose through changes in orbital forcing, CO_2 levels and other radiative forcing by way of interactions and feedbacks within the climate system. Nevertheless, it is not unexpected that the real world manifestation of a gradual change between states involving NADW formation being on or off would involve an intermediate period with fluctuations between the two states, much as occurred during the transition between the last glacial maximum and the present Holocene (e.g., the Younger Dryas—Fanning and Weaver, 1997a).
4. Model results are consistent with the hypothesis that the Late Pliocene extinction and speciation bioevent was caused by IP final closure. There are large differences between the tropical Atlantic and Pacific response. Other minor evolutionary events (e.g., snapping shrimp) have occurred throughout the gradual closure.

5. Model results showing increased AABW into the Pacific are consistent with the hypothesis, based on ODP and DSDP observations, that the Late Miocene carbonate crash was due to the initiation of NADW production.
6. Radiolarian data suggest changes in the location of the SEC, which may be related to IP closure. Model resolution is inappropriate for comparison to the location of the SEC. However, model results agree with observations of decreased eastern tropical Pacific temperature in the Miocene. They also support the idea that such results are not obtained for a similar location in the Pliocene because this response depended on closure to deep water.
7. Upwelling in the eastern tropical Pacific and off the east coast of Florida seems to be related to IP closure via a flow mechanism through the IP analogous to the Leeuwin current off Australia. This postulation cannot be verified directly due to model resolution, but indirect results are consistent with it. More intense AABW production modelled is consistent with increased AABW postulated as an explanation for observed upwelling changes.
8. A change in the characteristics of ENSO may have occurred anytime throughout IP closure. If so, it could have potentially had major effects on eastern Pacific biota and perhaps globally. Exactly what type of effects could have been expected to be attributed to such a change cannot be addressed at this time as studies are too preliminary to determine what differences in the character of ENSO would be expected with an open IP.
9. Model results lend weak support for Berggren's (1982) hypothesized mechanism connecting Northern Hemisphere glaciation in the Late Pliocene to IP closure. Suggestions were made for further modelling studies which may be able to more adequately address this question.

10. Sill depth experiments highlight the difficulty with reconstructing Isthmus closure. The non-linear response of the heat transport with decreasing sill depth arises because changes in thermohaline circulation strength (from changes in salinity homogenization—i.e., the magnitude of throughflow) act somewhat independently of changes in temperature in the basins (from changes in direction of throughflow at depth and at the surface). This fact, combined with the uncertainty in constraining closure, including possible intermittency of closure (§1.1), make the task of such a reconstruction virtually impossible. Much remains to be learned from increasingly sophisticated process-oriented sensitivity studies, but the focus should remain on sensitivity rather than simulation.

References

Allmon, W.D., S.D. Emslie, D.S. Jones, & G.S. Morgan, 1996, Late Neogene oceanographic change along Florida's west coast: Evidence and mechanisms, *Journal of Geology*, **104**, 143-162.

Axelrod, D.I., and P.H. Raven, 1985: Origins of the Cordilleran flora, *Journal of Biogeography*, **12**, 21-47.

Barnes, C., A. Hallam, D. Kaljo, E.G. Kauffman, and O.H. Walliser, 1995: Global Event Stratigraphy. In: *Global Events and Event Stratigraphy in the Phanerozoic*, Walliser, O.H. (Ed.), Springer, New York, pp. 173-224.

Berggren, W.A., 1982: Role of ocean gateways in climate change. In: *Climate in Earth history*, Berger, W.H. and J.C. Crowell (Eds.), National Academy Press, Washington, D.C., pp. 118-125.

Berggren, W.A. and C.D. Hollister, 1974: Paleogeography, paleobiogeography and the history of circulation in the Atlantic Ocean. In: *Studies in Paleooceanography*. Hay, W.W. (Ed.), Society of Economics, Paleontology and Mineralology Special Publication 20, pp. 126–186.

Blanc, T.V., 1987: Accuracy of bulk-method-determined flux, stability, and sea-surface roughness, *Journal of Geophysical Research*, **92**, 3867-3876.

Blanc, P.-L., D. Rabussier, C. Vergnaud-Grazzini, and J.-C. Duplessy, 1980: North Atlantic Deep Water formed by the middle Miocene, *Nature,* **283**, 553-555.

Bryden, H.L., 1993: Ocean heat transport across 24°N Latitude. In: *Interactions between global climate subsystems, the legacy of Hann.* Geophysical Monographs **75**, American Geophysical Union, pp 65-75.

Brunner, C., 1983/1984: Evidence for increased volume transport of the Florida Current in the Pliocene and Pleistocene, *Marine Geology*, **54**, 223-235.

Budyko, M.I., 1969: The effect of solar radiation variations on the climate of the earth, *Tellus*, **21**, 611–619.

Burbank, D.W., 1992: Causes of recent Himalayan uplift deduced from deposited patterns in the Ganges basin, *Nature*, **357**, 680-683.

Burton, K.W., H.-F. Ling, and R.K. O'Nions, 1997: Closure of the Central American Isthmus and its effect on deep-water formation in the North Atlantic, *Nature,* **386**, 382-385.

Coates, A.G., et al., 1992: Closure of the Isthmus of Panama: The near-shore marine record of Costa Rica and western Panama, *Geological Society America Bulletin,* **104**, 814-828.

Collins, L.S., A.F. Budd, and A.G. Coates, 1997: Earliest evolution associated with closure of the Tropical American Seaway: National Academy of Sciences Proceedings, in press.

Collins, L.S., A.G. Coates, W.A. Berggren, M.P. Aubry, and J. Zhang, 1996: The late Miocene Panama isthmian strait, *Geology,* **24**, 687-690.

Cronin, T.M., M.E. Raymo, and K.P. Kyle, 1996: Pliocene (3.2-2.4 Ma) ostracode faunal cycles and deep ocean circulation, North Atlantic Ocean, *Geology*, **24**, 695-698.

Crouch, R.W., and W.C. Poag, 1979: Amphistegina gibbosa D'Orbigny from the California borderlands: The Caribbean connection, *Journal of Foraminiferal Research*, **9**, 85-105.

Crowley, T.J. and G.R. North, 1991: *Paleoclimatology*. Oxford Monographs on Geology and Geophysics No. **18**, Oxford University Press, New York, 339 pp.

Delaney, M.L., 1990: Miocene benthic foraminifera Cd/Ca records: South Atlantic and western equatorial Pacific, *Paleoceanography*, **5**, 743-760.

Dowsett, H., J. Barron, R. Poore, 1996: Middle Pliocene sea surface temperatures: a global reconstruction, *Marine Micropaleontology*, **27**, 13-25.

Droxler, A., et. al., 1996: Caribbean constraints on circulation between Atlantic and Pacific Oceans over the last 40 Million Years. Submitted to: *Tectonic Boundary Conditions for Climate Reconstruction*, Oxford Monographs on Geology and Geophysics, eds. T. Crowley and K. Burke.

Duque-Caro, H. ,1990: Neogene stratigraphy, paleoceanography, and paleobiology in northwest South America and the evolution of the Panama seaway, *Paleogeography, Paleoclimatology, and Paleoecology*, **77**, 203-234.

Dutton, J.F. and E.J. Barron, 1997: Miocene to present vegetation changes: a possible piece of the Cenozoic cooling puzzle, *Geology*, **25**, 39-41.

Eyles, N., 1996: Passive margin uplift around the North Atlantic region and its role in Northern Hemisphere late Cenozoic glaciation, *Geology*, **24**, 103-106.

Fanning, A.F., 1997: Studies of the ocean-atmosphere system using a coupled climate model, Doctoral Thesis, University of Victoria, 174 pp.

Fanning, A.F. and A.J. Weaver, 1997a: Temporal-geographical meltwater influences on the North Atlantic Conveyor: Implications for the Younger Dryas, *Paleoceanography*, **12,** 307-320.

Fanning, A.F. and A.J. Weaver, 1997b: Thermohaline variability: the effects of horizontal resolution and diffusion, submitted to *Journal of Climate*

Fanning, A.F. and A.J. Weaver, 1997c: On the role of flux adjustments in an idealized coupled climate model, *Climate Dynamics,* in press.

Fanning, A.F. and A.J. Weaver, 1996: An atmospheric energy-moisture balance model: climatology, interpentadal climate change, and coupling to an OGCM. *Journal of Geophysical Research*, **101**, 15111-15128.

Filippelli, G.M., 1997: Intensification of the Asian monsoon and a chemical weathering event in the late Miocene-early Pliocene: implications for late Neogene climate change, *Geology*, **25**, 27-30.

Fischer, A.G., 1982: Long term climatic oscillations recorded in stratigraphy, In: *Climate in Earth history*, Berger, W.H. and J.C. Crowell (Eds.), National Academy Press, Washington, D.C., pp. 97-104.

Gartner, S., J. Chow, and R.J. Stanton, 1987: Late Neogene paleoceanography of the eastern Caribbean, the Gulf of Mexico, and the eastern equatorial Pacific, *Marine Micropaleontology*, **12**, 255-304.

Gates, W.L., A. Henderson-Sellers, G.J. Boer, C.K. Folland, A. Kitoh, B.J. McAvaney, F. Semazzi, N. Smith, A.J. Weaver, and Q.-C. Zeng, 1995: Climate Models - Evaluation. In: *Climate Change 1995: The Science of Climate Change, Contribution of Working Group I to the Second Assessment Report on the Intergovernmental Panel on Climate Change*, Houghton, J.T. et al. (Eds.), Cambridge University Press, pp. 229-284.

Gill, A.E., 1982: *Atmosphere-ocean dynamics*, Academic Press, New York, 662 pp.

Gore, R., 1997: The first steps, *National Geographic*, **191**, 72-97.

Graves, C.E., W.-H. Lee, and G.R. North, 1993: New parameterizations and sensitivities for simple climate models, *Journal of Geophysical Research*, **98**, no. D3, 5025-5036.

Haq, B.U., J. Hardenbol, and P.R. Vail, 1987: Chronology of fluctuating sea level since the Triassic (250 million years ago to present), *Science*, **235**, 1158-1167.

Haq, B.U., 1984, Paleoceanography: A synoptic overview of 200 Million years of ocean history. In: *Marine Geology and Oceanography of Arabian Sea and Coastal Pakistan*, Haq, B. & J. Milliman (Eds.), Van Nostrand Reinhold Company, pp. 201-231.

Hallam, A., 1977: Secular changes in marine inundation of USSR and North America through the Phanerozoic, *Nature*, **269**, 769-772.

Hoorn, C., J. Guerrero, G.A. Sarmiento, and M.A. Lorente, 1995: Andean tectonics as a cause for changing drainage patterns in Miocene northern South America, *Geology*, **23**, 237-240.

Isemer, H.J., J. Willebrand, and L. Hasse, 1989: Fine adjustment of large scale air-sea energy flux parameterizations by direct estimates of ocean heat transport, *Journal of Climate*, **2**, 1173-1184.

Jackson, J.B.C., P. Jung, A.G. Coates, and L.S. Collins, 1993: Diversity and extinction of tropical american mollusks and emergence of the Isthmus of Panama, *Science*, **260**, 1624-1626.

Kaneps, A.G., 1979: Gulf Stream: Velocity fluctuations during the Cenozoic, *Science*, **204**, 297–301.

Keigwin, L.D., 1982, Isotopic paleoceanography of the Caribbean and east Pacific: Role of Panama uplift in late Neogene time, *Science*, **217**, 350-353.

Keller, G., C.E. Zenker, and S.M. Stone, 1989: Late Neogene history of the Pacific-Caribbean gateway, *Journal of South American Earth Science,* **2**, 73-108.

Keller, G., and J.A. Barron, 1983: Paleoceanographic implications of Miocene deep-sea hiatuses, *Geological Society America Bulletin*, **94**, 590-613.

Kennett, J., 1982: *Marine Geology*, Prentice-Hall, Toronto, 813 pp.

Kling, S.A., 1978: Radiolaria. In: *Introduction to Marine Micropaleontology*, Haq, B.U., and A. Boersma (Eds.). Elsevier, New York, pp. 376.

Knowlton, N., L.A. Weight, L.A. Solorzano, D.K. Mills, and E. Bermingham, 1993: Divergence in proteins, mitochondrial DNA, and reproductive compatability across the Isthmus of Panama, *Science*, **260**, 1629-1632.

Knutson, T.R., S. Manabe, and D. Gu, 1997: Simulated ENSO in a global coupled ocean-atmosphere model: Multidecadal amplitude modulation and CO_2 sensitivity, *Journal of Climate,* **10**, 138-161.

Kutzbach, J.E., 1992: Modeling large climatic changes of the past. In: *Climate System Modeling*, Trenberth, K.E. (Ed.), Cambridge University Press, London, pp. 669–688.

Lindzen, R.S., and B. Farrell, 1977: Some realistic modifications of simple climate models, *Journal of Atmospheric Science*, **34**, 1487-1501.

Lorenz, E.N., 1979: Forced and free variations of weather and climate, *Journal of Atmospheric Science*, **36**, 1367-1376.

Luyendyk, B.P., D. Forsyth and J.D. Phillips, 1972: Experimental approach to the paleocirculation of the oceanic surface waters. *Geological Society America Bulletin.*, **83**, 2649–2664.

Lyle, M., K.A. Dadey, and J.W. Farrell, 1995: The Late Miocene (11-8 Ma) Eastern Pacific carbonate crash: evidence for reorganization of deep-water circulation by the closure of the Panama gateway, In: *Proceedings ODP, Scientific Results*, **138**: College Station TX. Pisias, N.G., L.A. Janecek, T.R. Palmer-Julson, and T.H. van Andel (Eds.), Ocean Drilling Program, pp. 821-838.

McDougall, K., 1996: Benthic foraminiferal response to the emergence of the Isthmus of Panama and coincident paleoceanographic changes, *Marine Micropaleontology*, **28**, 133-169.

Maier-Reimer, E., U. Mikolajewicz and T.J. Crowley, 1990: Ocean general circulation model sensitivity experiment with an open Central American Isthmus, *Paleoceanography*, **5**, 349–366.

Manabe, S., and R.J. Stouffer, 1988: Two stable equilbiria of a coupled ocean-atmosphere model, *Journal of Climate*, **1**, 841-866.

Marshall, L.G., 1985: Geochronoly and land-mammal biochronology of the transamerican faunal interchange. In: *The Great American Faunal Interchange*. Stehli, F.G. and S.D. Webb (Eds.), Plenum Press, New York, pp. 49-85.

Marshall. S.J., 1997: *UBC Ice sheet model documentation*, Dept. of Earth and Ocean Sciences, University of British Columbia, 51 pp.

Mikolajewicz, U., and T.J. Crowley, 1997: Response of a coupled ocean/energy balance model to restricted flow through the Central American Isthmus, *Paleoceanography,* in press.

Mikolajewicz, U., E. Maier-Reimer, T.J. Crowley and K.-Y. Kim, 1993: Effect of Drake and Panamanian gateways on the circulation of an ocean model, *Paleoceanography*, **8**, 409–426.

Miller, K.G., and R.G. Fairbanks, 1985: Oligocene and Miocene carbon isotope cycles and abyssal circulation changes. *In The Carbon cycle and atmospheric CO_2: Natural variations Archean to Present*, Geophysical Monographs **32**. Sundqvist, E.T. and W.S. Broecker (Ed.), American Geophysical Union, Washington, D.C., pp. 469-486.

Miller, K.G., and R.G. Tucholke, 1983: Development of Cenozoic abyssal circulation south of the Greenland-Scotland ridge. In: *The Carbon Cycle and Atmospheric CO_2: Natural Variations Archean to Present,* Geophysical Monographs **32**. Sundqvist, E.T. and W.S. Broecker (Ed.), American Geophysical Union, Washington, D.C., pp. 549-589.

Moore, T.C., Jr., and G. Lombardi, 1981: Sea surface temperature change in the North Pacific during the late Miocene, *Marine Micropaleontology*, **6**, 581-598.

Moore, T.C., Jr., N.G. Pisias, and N.J. Shackleton, 1993: Paleoceanography and the diachrony of radiolarian events in the eastern equatorial Pacific, *Paleoceanography*, **8**, 567-586.

Mullins, H.T., and A.C. Neumann, 1979: Geology of the Miami terrace and its paleoceanographic implications, *Marine Geology*, **30**, 205-232.

Murdock, T.Q., A.J. Weaver, and A.F. Fanning, 1997: Paleoclimatic response of the closing of the Isthmus of Panama in a coupled ocean-atmosphere model, *Geophysical Research Letters*, **24**, 253-256.

North, G.R., 1975: Theory of energy balance models, *Journal of Atmospheric Science*, **32**, 2033–2043.

Pacanowski, R., K. Dixon and A. Rosati, 1993: *The GFDL Modular Ocean Model User's Guide*, GFDL Ocean Group Technical Report #2, 46 pp.

Pujos, A., 1987, Mise en place de la circulation au Pacifique central equatorial et des assemblages des nannofossiles calcaires au Neogene, *Bulletin Societe Geologique France*, **4**, 731-736.

Raymo, M.E., D. Hodell, and E. Jansen, 1992: Response of deep ocean circulation to initiation of northern hemisphere glaciation (3-2 Ma), *Paleoceanography*, **7**, 645-672.

Rea, D.K., I.A. Basov, L.A. Krissek, and the Leg 145 Scientific Party, 1995: Scientific results of drilling in the North Pacific transect. In: Proceedings ODP, Scientific Results, 145. Rea, D.K., I.A. Basov, D.W. Scholl, J. Allan, et al. (Eds.). College Station TX, Ocean Drilling Program, pp. 577-596.

Reason, C.J.C., and S.B. Power, 1994: The influence of the Bering Strait on the circulation in a coarse resolution global ocean model, *Climate Dynamics*, **9**, 363-369.

Repenning, C.A., 1967: Subfamilies and genera of Soricidae, *U.S. Geological Survey Professional Paper,* **565**.

Ruddiman, W.F., A. McIntyre, V. Niebler-Hunt, and J.T. Durazzi, 1980: Oceanic evidence for the mechanism of rapid Northern Hemisphere glaciation, *Quaternary Research*, **13**, 33-64.

Sancetta, C.A., 1983: Biostratigraphic and paleoceanographic events in the eastern equatorial Pacific: Results of Deep Sea Drilling Project Leg 69. In: *Initial Repts., DSDP,* **69**. Cann, J.R. et al. (Eds.). Washington, U.S. Gov't Printing Office, pp. 311-319.

Semtner, A.J., 1976: A model for the thermodynamic growth of sea ice in numerical investigations of climate, *Journal of Physical Oceanography*, **6**, 379-389.

Stanley, S.M., 1996: Children of the ice age: How a global catastrophe allowed humans to evolve, Harmony Books, 250 pp.

Sykes, L.R., W.R. McCann, and A.L. Kafka, 1982: Motion of the Caribbean plate during the last 7 million years and implications for earlier Cenozoic movements, *Journal of Geophysical Research*, **87**, 10656-10676.

Svitil, K.A., 1993: Ocean divided, *Discover*, **14**, 38-39.

Talley, L.D., 1984: Meridional heat transport in the Pacific Ocean, *Journal of Physical Oceanography*, **14**, 231-241.

Thompson, S.L., and S.G. Warren, 1982: Parameterization of outgoing infrared radiation derived from detailed radiative calculations, *Journal of Atmospheric Science*, **39**, 2667-2680.

Vermeij, G. J.,1993: Biological history of a seaway, *Science*, **260**, 1603-1604.

Vermeij, G.J., 1989: An ecological crisis in an evolutionary context: El-Nino in the eastern Pacific. In: Global ecological consequences of the 1982-83 El Nino-Southern Oscillation. Glynn, P.W. (Ed.). Elsevier, Amsterdam.

Vermeij, G.J., & E.J. Petuch, 1986, Differential extinction in tropical american mollusks: endemism, architecture, and the Panama land bridge, Malacologia, 27(1), 29-41.

Warren, B.A., 1983: Why is there no deep water formed in the North Pacific?, *Journal of Marine Research*, **41**, 327-347.

Weaver, A.J., 1990: Ocean currents and climate, *Nature*, **347**, 432.

Weaver, A.J. and T.M.C. Hughes, 1996: On the incompatibility of ocean and atmosphere models and the need for flux adjustments, *Climate Dynamics*, **12**, 141–170.

Wijffels, S.E., R.W. Schmitt, H.L. Bryden and A. Stigebrandt, 1992: Transport of freshwater by the oceans, *Journal of Physical Oceanography*, **22**, 155–162.

Wold, C.N., 1994: Cenozoic sediment accumulation on drifts in the northern North Atlantic, *Paleoceanography*, **9**, 917-941.

Woodruff, F., and S.M. Savin, 1989: Miocene deepwater oceanography, *Paleoceanography,* **4**, 87-140.

Wright, J.D., and K.G. Miller, 1996: , Control of North Atlantic Deep Water circulation by the Greenland-Scotland Ridge, *Paleoceanography*, **11**, 157-170.

Wright, J.D., K.G. Miller and R.G. Fairbanks, 1992: Early and middle Miocene stable isotopes: Implications for deepwater circulation and climate, *Paleoceanography*, **7**, 357-389.

Wright, J.D., K.G. Miller and R.G. Fairbar dern deepwater circulation: Evidence from the Late Miocene southern ocean, *Paleoceanography*, **6**, 275-290.

VITA

Surname: Murdock Given Names: Trevor Quentin
Place of Birth: Trail, BC, Canada

Educational Institutions Attended:

Danderyds Gymnasium	1989-90
Malaspina College	1990-91
University of Victoria	1991-97

Degrees Awarded:

B.Sc. (Honours Co-op with Distinction)	University of Victoria	1995

Honours and Awards:

NSERC Postgraduate Scholarship	Declined	1997
UVic Graduate Research Fellowship	University of Victoria	1996-97
NSERC Undergraduate Award	University of Victoria	1995
Dorothy Harper Memorial Scholarship	University of Victoria	1994-95
Molson Companies Scholarship	University of Victoria	1994-95
B.W. Pearse Science Scholarship	University of Victoria	1994-95
J. L. Climenhaga Scholarship	University of Victoria	1993-94
Seaspan Scholarship	University of Victoria	1993-94
President's Entrance Award	University of Victoria	1991-92
Canada Scholarship	Malaspina/UVic	1990-95
John Locke Malkin Scholarship	Malaspina College	1990-91
B.C. Provincial Scholarship	Malaspina College	1990-91
Reader's Digest Academic Scholarship	Malaspina College	1990-91
Rotary Academic Scholarship	Malaspina College	1990-91
Passport to Education	Malaspina College	1990-91
Sweden Academic Achievement Award	Danderyds Gymnasium	1989-90

Publications:

Barnes, J.A., T.E. Gough, T.Q. Murdock, and M. Stoer, 1995: Absolute Intensities in Photo-acoustic Spectroscopy, *Review of Scientific Instruments*, **67**, F '96, 371-4.

Murdock, T.Q., A.J. Weaver, and A.F. Fanning, 1997: Paleoclimatic response of the closing of the Isthmus of Panama in a coupled ocean-atmosphere model. *Geophysical Research Letters*, **24**, 253-256.

PARTIAL COPYRIGHT LICENSE

I hereby grant the right to lend my thesis to users of the University of Victoria Library, and to make single copies only for such users or in response to a request from the Library of any other university, or similar institution, on its behalf or for one of its users. I further agree that permission for extensive copying of this thesis fpr scholarly purposes may be granted by me or a member of the University designated by me. It is understood that copying or publication of this thesis for financial gain shall not be allowed without my written permission.

Title of Thesis:

Paleoclimatic Response of the Closure of the Isthmus of Panama in a Coupled Ocean-Atmosphere Model

Author 

Trevor Quentin Murdock

September 5, 1997